



OPEN ACCESS

EDITED BY

Elena E. Grigorenko,
Space Research Institute (RAS), Russia

REVIEWED BY

Alexei V. Dmitriev,
Lomonosov Moscow State University,
Russia
Lauri Holappa,
University of Oulu, Finland

*CORRESPONDENCE

Kyle R. Murphy,
✉ kylemurphy.spacephys@gmail.com

SPECIALTY SECTION

This article was submitted to
Space Physics,
a section of the journal
Frontiers in Astronomy and
Space Sciences

RECEIVED 05 January 2023

ACCEPTED 07 February 2023

PUBLISHED 22 February 2023

CITATION

Sibeck DG, Murphy KR, Porter FS,
Connor HK, Walsh BM, Kuntz KD, Zesta E,
Valek P, Baker CL, Goldstein J, Frey H,
Hsieh S-Y, Brandt PC, Gomez R,
DiBraccio GA, Kameda S, Dwivedi V,
Purucker ME, Shoemaker M, Petrinec SM,
Aryan H, Desai RT, Henderson MG,
Cucho-Padin G and Cramer WD (2023),
Quantifying the global solar wind-
magnetosphere interaction with the
Solar-Terrestrial Observer for the
Response of the Magnetosphere
(STORM) mission concept.
Front. Astron. Space Sci. 10:1138616.
doi: 10.3389/fspas.2023.1138616

COPYRIGHT

© 2023 Sibeck, Murphy, Porter, Connor,
Walsh, Kuntz, Zesta, Valek, Baker,
Goldstein, Frey, Hsieh, Brandt, Gomez,
DiBraccio, Kameda, Dwivedi, Purucker,
Shoemaker, Petrinec, Aryan, Desai,
Henderson, Cucho-Padin and Cramer.
This is an open-access article distributed
under the terms of the [Creative
Commons Attribution License \(CC BY\)](#).
The use, distribution or reproduction in
other forums is permitted, provided the
original author(s) and the copyright
owner(s) are credited and that the original
publication in this journal is cited, in
accordance with accepted academic
practice. No use, distribution or
reproduction is permitted which does not
comply with these terms.

Quantifying the global solar wind-magnetosphere interaction with the Solar-Terrestrial Observer for the Response of the Magnetosphere (STORM) mission concept

David G. Sibeck¹, Kyle R. Murphy^{2,3*}, F. Scott Porter¹,
Hyunju K. Connor¹, Brian M. Walsh⁴, Kip D. Kuntz⁵, Eftyhia Zesta¹,
Phil Valek⁶, Charles L. Baker¹, Jerry Goldstein⁶, Harald Frey⁷,
Syau-Yun Hsieh⁸, Pontus C. Brandt⁸, Roman Gomez⁶,
Gina A. DiBraccio¹, Shingo Kameda⁹, Vivek Dwivedi¹,
Michael E. Purucker¹, Michael Shoemaker¹, Steven M. Petrinec¹⁰,
Homayon Aryan¹¹, Ravindra T. Desai¹², Michael G. Henderson¹³,
Gonzalo Cucho-Padin^{1,14} and W. Douglas Cramer¹⁵

¹NASA/GSFC, Greenbelt, MD, United States, ²Independent Researcher, Thunder Bay, ON, Canada, ³Department of Maths, Physics and Electrical Engineering, Northumbria University, Newcastle Upon Tyne, United Kingdom, ⁴Department of Mechanical Engineering and Center for Space Physics, Boston University, Boston, MA, United States, ⁵Johns Hopkins University, Baltimore, MD, United States, ⁶Southwest Research Institute, San Antonio, TX, United States, ⁷Space Sciences Laboratory, University of California, Berkeley, CA, United States, ⁸Johns Hopkins University Applied Physics Laboratory, Laurel, MD, United States, ⁹Department of Physics, College of Science, Rikkyo University, Tokyo, Japan, ¹⁰Lockheed Martin ATC, Palo Alto, CA, United States, ¹¹Atmospheric and Oceanic Sciences, University of California Los Angeles, Los Angeles, CA, United States, ¹²Centre for Fusion, Space and Astrophysics, University of Warwick, Coventry, United Kingdom, ¹³Space Science and Applications Group, Los Alamos National Laboratory, Los Alamos, NM, United States, ¹⁴Catholic University of America, Washington, DC, United States, ¹⁵Space Science Center University of New Hampshire, Durham, NH, United States

Much of what we know about the solar wind's interaction with the Earth's magnetosphere has been gained from isolated *in-situ* measurements by single or multiple spacecraft. Based on their observations, we know that reconnection, whether on the dayside magnetopause or deep within the Earth's magnetotail, controls the bulk flow of solar wind energy into and through the global system and that nightside activity provides the energized particles that power geomagnetic storms. But by their very nature these isolated *in-situ* measurements cannot provide an instantaneous global view of the entire system or its cross-scale dynamics. To fully quantify the dynamics of the coupled solar wind-magnetosphere requires comprehensive end-to-end global imaging of the key plasma structures that comprise the magnetosphere which have spatial resolutions that exceeds anything possible with multi-point or constellation *in-situ* measurements. Global, end-to-end, imaging provides the pathway to understanding the system as a whole, its constituent parts, and its cross-scale processes on a continuous basis, as needed to quantify the flow of solar wind energy through the global magnetospheric system. This paper describes how a comprehensively-instrumented single spacecraft in a high-altitude, high-

inclination orbit coupled with ground-based instruments provides the essential observations needed to track and quantify the flow of solar wind energy through the magnetosphere. This includes observations of the solar wind plasma and magnetic field input, the magnetopause location in soft X-rays, the auroral oval in far ultraviolet, the ring current in energetic neutrals, the plasmasphere in extreme ultraviolet, the exosphere in Lyman- α , and the microstructure of the nightside auroral oval from ground-based all sky cameras.

KEYWORDS

solar wind-magnetosphere interaction, global imaging, mission concept, soft X rays, aurora, ring current, plasma sphere

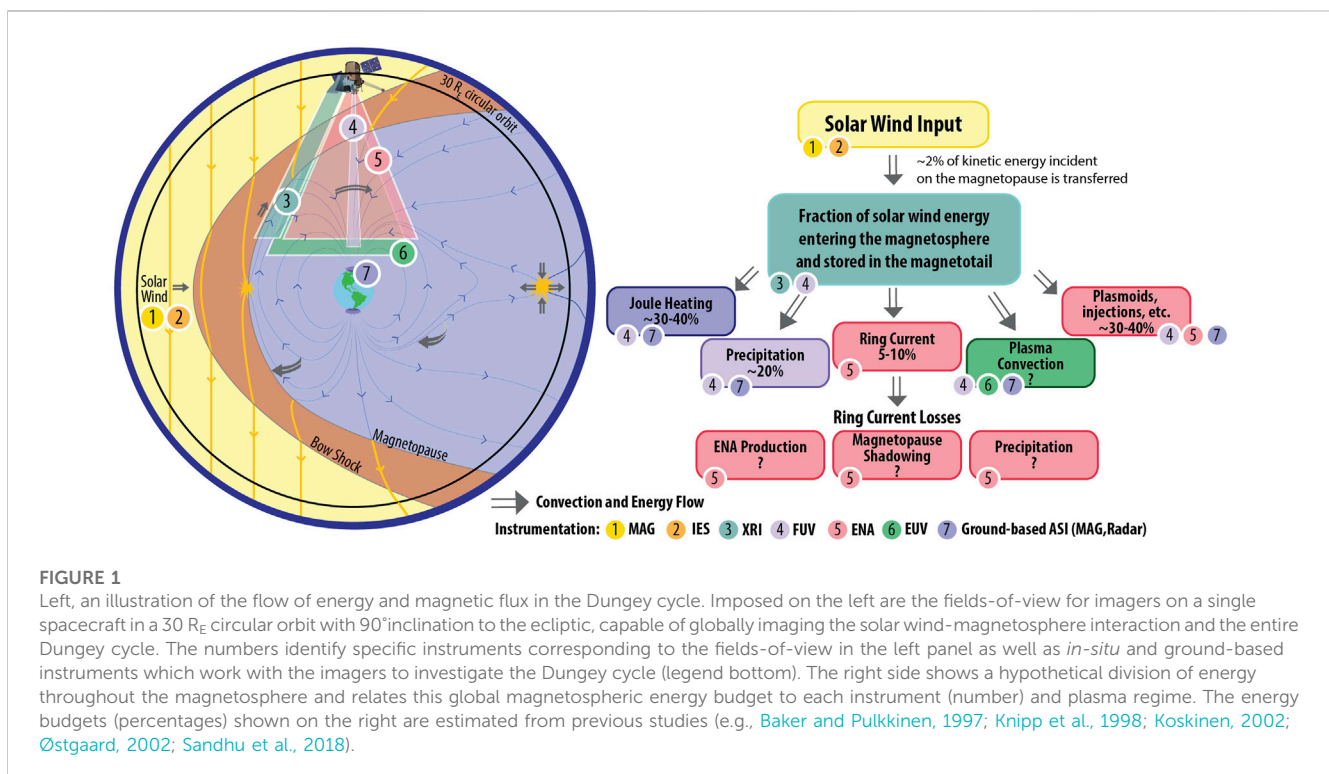
1 Introduction

Magnetic reconnection is the process that enables most solar wind energy to enter and flow through the magnetosphere. At the dayside magnetopause reconnection occurs when interplanetary and terrestrial magnetic fields merge creating open magnetic field lines which allows solar wind mass, energy, and momentum to cross the magnetopause and enter the magnetosphere. The solar wind drags the ionospheric ends of these open magnetic field lines across the polar cap and stretches the magnetic field lines to form the Earth's nightside magnetotail where magnetic flux is stored. Magnetic reconnection within the nightside plasma sheet closes the stored flux, sends streams of particles and powerful field-aligned currents down into the nightside auroral oval, and injects plasma sheet ions and electrons into the Earth's inner magnetosphere and in particular the ring current and radiation belts. Nightside reconnection returns closed magnetic field lines and cold plasma to the dayside magnetosphere *via* convection, upon which this sequence of events, known as the Dungey Cycle (Dungey, 1961),

begins anew. This cycle is illustrated in the left-hand panel of Figure 1. Only a fraction of the incident solar wind's energy enters the magnetosphere *via* dayside reconnection. However, this small fraction suffices to drive the complex spatiotemporal dynamics of the coupled solar wind-magnetosphere system, powering space weather, the aurora, and the acceleration and dynamics of plasma throughout the magnetosphere (Figure 1 right).

The holistic view described above and our overall understanding of the solar wind-magnetosphere interaction, the circulation of energy through the system, and the physical processes which control this interaction and circulation (Figure 1 right) has been pieced together from sparse *in-situ* observations. Over many years, we have observed parts of this complex system in a piecemeal manner, but a complete system level view from start (at the dayside boundary) to finish (in the inner magnetosphere and ionosphere) remains missing.

In this paper we expand on the decadal white paper "Imaging the End-to-End Dynamics of the Global Solar Wind-Magnetosphere Interaction" which describes the utility of a global imaging mission



for addressing system science of the solar wind-magnetosphere interaction depicted in Figure 1. In particular, we detail the Solar Terrestrial Observer for the Response of the Magnetosphere (STORM) mission concept. STORM globally images the plasma regimes critical to the transfer and circulation of energy in the solar wind-magnetosphere system as well as the solar wind input into the system. In this way the STORM mission concept is a paradigm shift from current missions which rely on isolated local *in-situ* observations to a set of simultaneous remote sensing and *in-situ* observations which characterize and quantify the dynamics of the entire solar wind-magnetosphere system—a strategic system science approach. In the following sections we describe the STORM mission concept in detail including; mission design, objectives and observation requirements (by objective), and discuss the STORM mission concept in the context of the current state of the heliophysics field.

2 Mission design

The Solar Terrestrial Observer for the Response of the Magnetosphere (STORM) mission is a global imaging mission whose overarching science goal is to quantify the solar wind-magnetosphere interaction. From a circular $30 R_E$ orbit inclined 90° to the ecliptic, STORM simultaneously observes the solar wind input into the magnetosphere and comprehensively images the response of magnetospheric plasma structures on time scales ranging from minutes to days and on spatial scales ranging from km to multiple Earth radii (R_E) (Figure 1 right). As shown in Figure 1 specific STORM targets include: the solar wind plasma (orange) and interplanetary magnetic field (IMF, yellow), which quantifies the energy input to the magnetosphere system; the dayside magnetopause (teal), where reconnection enables solar wind energy to enter the magnetosphere; the auroral oval (purple), with expansions and contractions that define energy storage within the magnetotail; the magnetotail, where this stored energy is released by reconnection; the ring current (red), which receives much of the stored energy in the form of accelerated ions; and the plasmasphere (green) which stores the bulk of cold plasma in the magnetosphere. STORM comprehensively tracks the end-to-end circulation of energy throughout the solar wind-magnetosphere system by systematically addressing four sequentially linked science objectives investigating the relative changes in the magnetosphere energy budget:

- (1) energy transfer at the dayside magnetopause
- (2) energy circulation and transfer through the magnetotail
- (3) energy sources and sinks for the ring current
- (4) energy feedback from the inner magnetosphere.

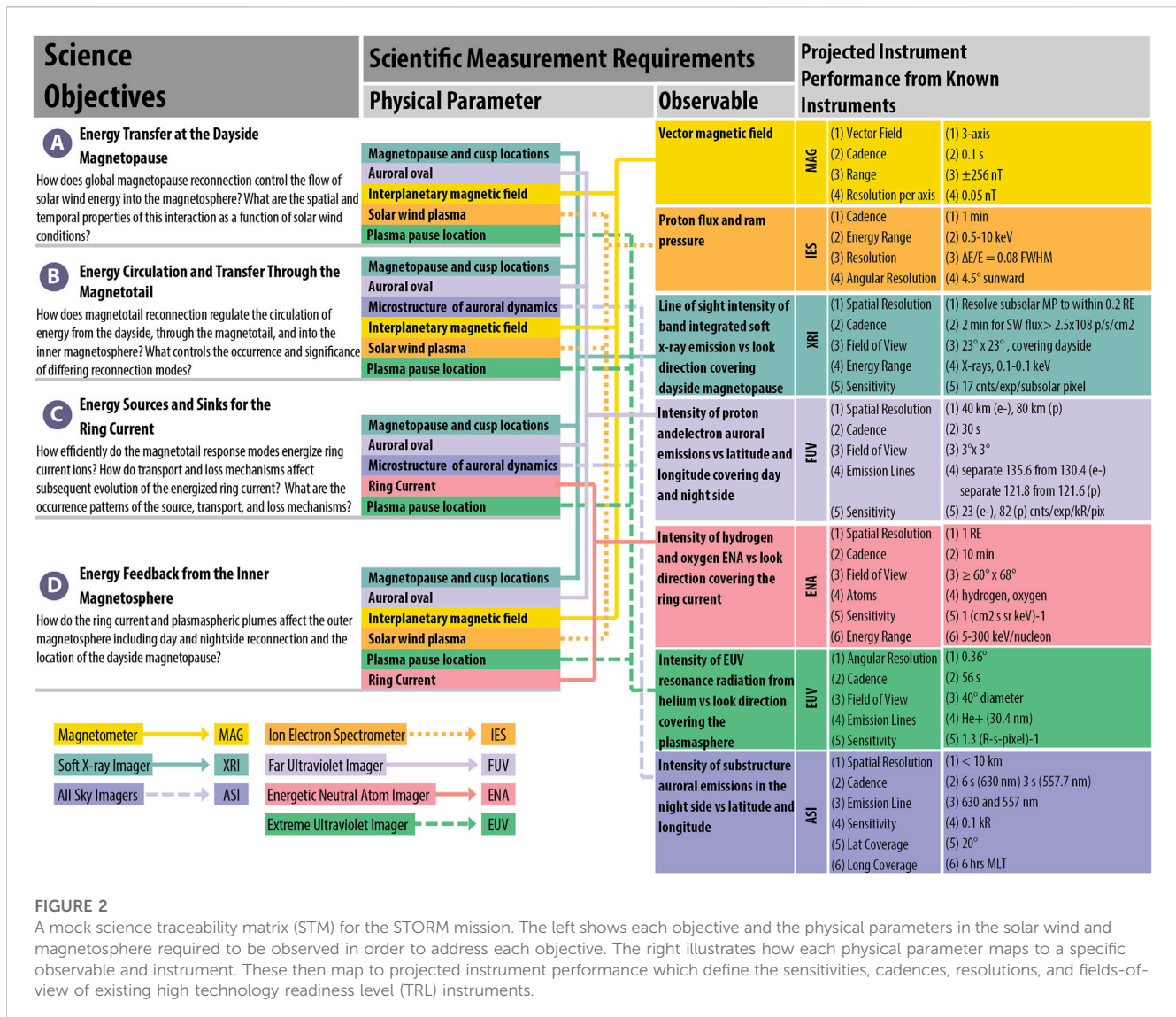
STORM achieves these objectives with a comprehensive instrument payload that combines multispectral and neutral atom magnetospheric imaging with nearby solar wind monitoring. STORM's primary instrument, the soft X-ray imager (XRI), captures global images of the dayside magnetosheath and its boundaries from the soft X-rays generated when high-charge-state solar wind ions encounter exospheric neutrals (Sibeck et al., 2018). XRI tracks the location of the magnetopause to determine the

global spatiotemporal properties of reconnection at this boundary and its response to solar wind, magnetotail, and inner magnetosphere conditions never before possible with either single point or constellation *in-situ* missions such as MMS (Sibeck et al., 2018). The Far Ultraviolet (FUV) spectrographic telescope images proton and electron aurora to identify, distinguish between, and quantify the significance of modes of magnetopause reconnection, magnetotail reconnection, and ring current ion precipitation. A dedicated array of ground-based All-Sky Imagers (ASI) distributed strategically throughout Canada and Alaska complements FUV by providing the high-fidelity time and spatial observations needed to track the development of the nightside auroral microstructures thought to precede substorm onset. The Energetic Neutral Atom (ENA) camera takes unprecedented images of plasma sheet and ring current ion transport, energization, and loss central to the flow of energy into, through, and out from the inner magnetosphere. The Extreme Ultraviolet (EUV) imager tracks the plasmapause to quantify the convection that occurs in response to dayside and nightside magnetotail reconnection modes, identifies locations where wave-particle interactions may drive ring current ion precipitation, and determines when and where plasmaspheric plumes may affect dayside reconnection.

Capturing global images of the magnetosphere's plasma morphology from all perspectives requires a highly-inclined circular 9.65 day orbit at a $\sim 30 R_E$ radial distance that precesses through all local times. The orbit is stable enough to maintain its nearly circular shape for several years, even in the presence of luni-solar gravitational perturbations, without requiring orbit station-keeping maneuvers. The transfer trajectory design uses a lunar gravity assist to change the inclination into the desired value of 90° relative to the ecliptic, which enables the mission to be achieved with a modestly sized launch vehicle. Lastly, the science orbit will naturally decay at the end of the mission due to dynamic coupling between the luni-solar gravity, enabling an atmospheric disposal strategy without requiring additional maneuvers.

From this $\sim 30 R_E$ stable vantage point, STORM can make its own uninterrupted and simultaneous observations of the solar wind input and the magnetospheric response throughout the course of interaction modes such as geomagnetic storms and steady convection events that can last for multiple days. Consequently, STORM's payload includes the Ion Electron Spectrometer (IES) and a magnetometer (MAG) to observe the solar wind plasma and IMF input. By observing the solar wind from locations well outside the bow shock but still in Earth's vicinity, STORM determines the solar wind input to the magnetosphere with a certainty better than observations propagated from any L1 monitor (Shoemaker et al., 2022).

STORM's imagers comprehensively identify and track the locations and motion of magnetospheric structures and boundaries: the magnetopause (XRI), the auroral oval (FUV) and its microstructure (ASI), the ring current (ENA), and plasmasphere (EUV). XRI tracks the eroding dayside magnetopause to determine global dayside reconnection rates. FUV complements this task by specifying dayside reconnection rates from cusp auroral intensities and the latitudinal motion of the dayside auroral oval. FUV tracks the poleward moving nightside auroral oval to quantify the nightside flux closed by different magnetotail response modes specified by ASI. XRI and ENA determine ring current loss *via* ion outflow



through the magnetopause, FUV and ENA quantify ion loss *via* precipitation at subauroral latitudes, while ENA directly observes ring current ion loss *via* charge exchange. EUV tracks the dynamic plasmasphere and plasmaspheric plumes to diagnose the effect of cold plasma on dayside reconnection and quantify changes in the strength of convective electric fields. Figure 2 illustrates STORM’s mock science traceability matrix (STM), tracing each of STORM’s objectives to a measurement requirement including physical parameter and observable, and to projected instrument performance. STORM’s objectives, and measurement requirements are described in the next section.

Though not part of STORM’s core mission, a Lyman- α imager, and ground-based magnetometers and radars offer additional utility to the STORM mission. Charge exchange of singly-charged hydrogen and oxygen with exospheric neutrals produce the ENA signatures that diagnose the ring current and inner plasma sheet conditions, whereas charge exchange of multiply-charged heavier atoms in the solar wind with exospheric neutrals produces the soft X-ray signals that diagnose the locations of the magnetopause and

high-altitude cusps. A Lyman- α imager, like Lyman-Alpha Imaging Camera (LAICA) onboard the PROCYON spacecraft (Kameda et al., 2017), allows STORM to quantify the three-dimensional distribution of exospheric neutral densities and subsequently discern plasma distributions within the ring current (coupled with ENA) and magnetosheath (coupled with XRI). Arrays of ground-based magnetometers and radars at high latitudes, of the type already existing across Alaska, Canada, and Scandinavia further supplement STORM allowing the determination of field aligned currents, the ionospheric counterpart of the magnetospheric convective electric field, and magnetic field perturbations associated with day and nightside reconnection.

3 Science objectives and requirements

STORM addresses its overarching science goal by completing four science objectives (and subquestions, Figure 2). The measurements required to complete these objectives and achieve

STORM's science goals are detailed here and in the mock STM shown in Figure 2. Sections 3.1–3.4 describe each of the four science objectives, provide background about the unanswered questions, describe how STORM distinguishes between proposed interaction modes, describe how STORM determines the occurrence patterns for each mode, and demonstrate how STORM quantifies the significance of each mode to the overall solar wind-magnetosphere interaction.

3.1 Science objective A: Energy transfer at the dayside magnetopause

Energy transfer between the solar wind and Earth's magnetosphere at the dayside magnetopause is the first step in the Dungey cycle and subsequent circulation of energy through the coupled solar wind-magnetosphere system. As part of Science Objective A, STORM answers two fundamental science questions: 1) How does global magnetopause reconnection control the flow of solar wind energy into the magnetosphere? 2) What are the spatial and temporal properties of this interaction as a function of solar wind conditions?

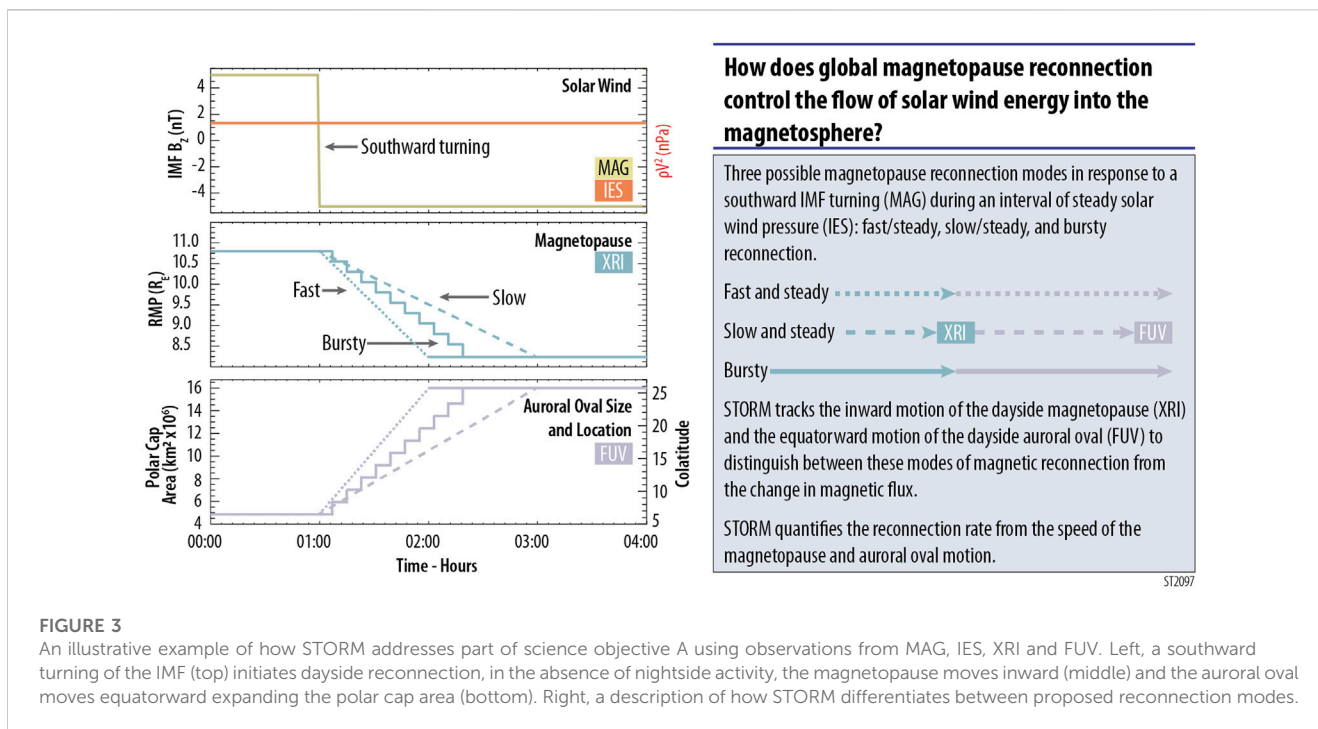
Understanding the dynamics of reconnection is essential to quantifying the flow of energy in the solar wind-magnetosphere interaction. Global simulations, *in-situ*, and remote measurements provide evidence for different magnetopause reconnection modes. Reconnection can be steady (Sonnerup et al., 1981; Trattner et al., 2021) or bursty (Russell & Elphic, 1978; Pfau-Kempf et al., 2020; Zou et al., 2022), and may (Lockwood et al., 1989) or may not (Le et al., 1993) be triggered by southward IMF turnings. Reconnection can be localized to less than 1 h of local time (Marchaudon et al., 2004; Oksavik et al., 2004; Oksavik et al., 2005; Fear et al., 2007) or extend across 5–8 h of local time on the dayside magnetopause (Lockwood et al., 1990; Milan et al., 2016), it may occur at off-equatorial pre- and post-noon (Crooker, 1979; Sandholt and Farrugia, 2003) or subsolar locations (Sonnerup, 1974; Mozer et al., 2002). Reconnection at the dayside magnetopause can take place gradually over 1–2 h causing an earthward erosion of the magnetopause of 1–2 R_E (Aubry et al., 1970) and an equatorward motion of the cusp aurora of more than 8° (~800 km in the auroral oval) (Burch, 1972). This corresponds to a protracted interval of localized dayside proton precipitation resulting in auroral intensities of 1 kR, with a longitudinal width of $\sim 10^\circ$ (~290 km) that can move 3 h in local time over a few hours (Frey et al., 2003; Phan et al., 2003). Alternatively, reconnection may take place abruptly in ~ 1 – 3 min bursts each ~ 7 – 10 min that generate flux transfer events with dimensions $\sim 1 R_E$ normal to the magnetopause (Russell and Elphic, 1978). This leads to recurrent auroral brightenings followed by the equatorward motion of the dayside auroral oval in 100 km steps (Sandholt et al., 1998) and corresponding earthward and equatorward jumps of the magnetopause and cusp.

STORM distinguishes between steady and unsteady modes of magnetopause reconnection by tracking the motion of the magnetopause (XRI), dayside auroral oval (FUV), and intensity of proton auroral precipitation (FUV). To capture the location of the subsolar magnetopause over a broad range of solar wind conditions equivalent to a 5.2 R_E range of magnetopause locations from its canted location on STORM some 30 R_E from Earth, XRI requires a

$10^\circ \times 10^\circ$ field of view (FOV). To distinguish between steady and unsteady reconnection and erosion of the magnetopause, XRI must track spatiotemporal variations in the density gradients that indicate lines of sight tangent to the magnetopause with the 0.25 R_E and 3 min resolution needed to track 1–2 R_E erosion of the magnetopause (Aubry et al., 1970) over 60–120 min. From some vantage points, STORM would observe lines of sight that lie tangent to locations near the subsolar magnetopause; however, lines of sight tangent to the magnetopause away from the subsolar point can just as readily be used to identify magnetopause motion and determine the global spatiotemporal dependence of magnetic reconnection on the orientation of the interplanetary magnetic field (Collier and Connor, 2018). To quantify the spatial and temporal dynamics of reconnection, FUV must track the latitude of the dayside auroral oval with 100 km resolution and 3 min cadence to distinguish between magnetopause reconnection modes that drive 8° motion (Burch, 1972) over 60–120 min. FUV must also observe the intensity of the proton aurora with a spatial resolution and cadence of 100 km and 3 min to distinguish between proton precipitation driven by steady and unsteady dayside reconnection (Frey et al., 2003). The cadences and spatial resolutions for the XRI and FUV imagers readily distinguish between modes of dayside reconnection (Figure 2).

STORM employs FUV observations to infer the location and extent of magnetic reconnection on the magnetopause. FUV must track the location and azimuthal extent of latitudinal motion in the electron auroral oval with a 100 km resolution to determine the azimuthal extent and flux opened by bursty reconnection and whether it is confined to the vicinity of local noon or occurs preferentially at locations away from local noon to distinguish between component and antiparallel reconnection models (Milan et al., 2000). Similarly, FUV must identify the locations where proton aurora occurs within the dayside auroral oval with a spatial resolution and cadence of at least 100 km (3.5° longitude at 75° cusp latitudes) to determine the extent and location of the reconnection line (component vs antiparallel) as projected into the ionosphere from observations of proton precipitation (Frey et al., 2003; Lockwood et al., 2003).

STORM's *in-situ* measurements of the solar wind determine event occurrence patterns. IES must observe the local solar wind plasma input with a cadence of 2 min, commensurate with that of the magnetospheric imagers, to accurately identify the arrival times of solar wind features at the subsolar magnetopause, eliminate solar wind dynamic pressure variations as the cause of magnetopause motion and changes in the brightness of the dayside aurora, and identify signatures in the solar wind plasma that may trigger reconnection (Frey et al., 2019). MAG must observe the IMF with a cadence of 1.5 s or faster to employ cross-product and minimum variance algorithms that determine the locations where solar wind features first impact the magnetosphere and trigger reconnection with less uncertainty than observations from L1 (Crooker et al., 1982; Cameron and Jackel, 2016). Finally, the EUV must observe the ~ 1 – $1.8 R_E$ sunward motion of the day and nightside plasmasphere over >60 min (Goldstein et al., 2003; Goldstein and Sandel, 2005), readily observable with the 0.18 R_E spatial resolution and 2 min cadence of EUV. This motion quantifies the changes in the strength of convective electric fields in the inner magnetosphere associated with dayside reconnection providing an



additional diagnosis of the significance of different reconnection modes in the solar wind-magnetosphere interaction.

STORM's mission design provides multiple ways to quantify the significance of individual dayside reconnection events: 1) *via* direct observations of the intensity and extent of the dayside proton aurora (Frey et al., 2003), 2) *via* the amount of dayside flux opened by equatorward motion of the electron auroral oval, 3) *via* the amount of flux eroded from the dayside magnetosphere as inferred from observations of eroding magnetopause locations and 4) *via* inferences of the dayside reconnection electric field imposed on the inner magnetosphere from observations of low energy plasmaspheric motion. Statistical studies determine the geomagnetic effectiveness of each dayside reconnection mode as a function of solar wind drivers and geomagnetic conditions. Requirements for XRI and FUV are the same as those listed above. FUV must be capable of continuously observing the location, extent, and intensity of the dayside auroral oval and proton aurora over days, corresponding to the time scale of geomagnetic storms (Lockwood et al., 2003; Frey, 2007; Milan et al., 2007).

STORM's comprehensive global space-based observations 1) identify distinct modes of magnetopause reconnection, 2) determine their occurrence patterns, and 3) quantify their significance in the circulation of energy throughout the magnetosphere as a function of solar wind and geomagnetic conditions providing science closure to objective A. Figure 3 presents an idealized example of how STORM discriminates between modes of dayside reconnection thereby quantifying the physical processes governing the entrance of energy into the solar wind magnetosphere system. It is noteworthy to mention that though Figure 3 is an idealized example, the STORM team has developed algorithms to identify the magnetopause boundary which take into account both XRIs instrument response as well as background noise (Sibeck et al.,

2018). Similarly, the team has been working with existing algorithms developed during the IMAGE era (Boakes et al., 2008; Milan et al., 2009a) to improve the identification of auroral features and boundaries with the FUV instrument. Other researchers have also been developing algorithms to identify the magnetopause from simulated soft X-ray instruments (Collier & Connor, 2018; Jorgensen et al., 2019a; Jorgensen et al., 2019b; Sun et al., 2020; Connor et al., 2021). Finally, the STORM team combines observations from FUV and XRI to separate magnetopause motion driven by reconnection and that driven by changes in solar wind dynamic pressure.

3.2 Science objective B: Energy circulation and transfer through the magnetotail

Following dayside magnetopause reconnection, open magnetic flux is transported over the polar cap and stored within the magnetotail. This flux does not build up indefinitely. Eventually reconnection is triggered within the nightside plasma sheet. Reconnection closes the open magnetic flux and accelerates closed magnetic flux and plasma into the inner magnetosphere. Science objective B addresses this energy circulation and transfer through the magnetotail by answering two key questions: 1) How does magnetotail reconnection regulate the circulation of energy from the dayside, through the magnetotail, and into the inner magnetosphere? 2) What controls the occurrence and significance of differing reconnection modes?

In-situ and remote measurements, together with supporting results from global simulations, provide evidence for a number of distinct magnetotail reconnection modes (DeJong et al., 2007; Kissinger et al., 2012a; Walach et al., 2017) that cannot be deconvolved without observing the complete system. This

TABLE 1 A synthesis of triggers for nightside response modes, ●—trigger, ○—does not trigger. The large number and variety of proposed drivers for nightside response modes demonstrate the need for STORM which images the global solar wind-magnetosphere interaction and will determine the conditions under which these modes occur.

Nightside mode	Driver	Action and reference	Observers
Substorm onset	Auroral Streamers	●—Lyons et al. (2010), Nishimura et al. (2011)	FUV, ASI
	Pressure increase	●—Burch (1972), Lyons et al. (2005), Schiedge and Siscoe (1970)	IES, FUV, ASI
	Northward IMF turning	●—Caan et al. (1978), Gallardo-Lacourt et al. (2012), Hsu (2002), Rostoker (1983)	MAG, FUV, ASI
		○—Freeman and Morley (2004), Newell and Liou (2011)	
	IMF Bx reversal	●—Nowada et al. (2012)	MAG, FUV, ASI
	Open flux threshold	●—Boakes et al. (2009)	FUV, ASI
	Enhanced plasma sheet temperature	●—Forsyth et al. (2014)	ENA, FUV, ASI
	Enhanced O+	●—Baker et al. (1985)	ENA, FUV, ASI
○—Fok et al. (2006), Grande et al. (1999)			
Intense and storm-time substorms	High solar wind velocity	●—Pulkkinen et al. (2007)	IES, FUV, ASI
	High solar wind pressure	●—Vorobjev et al. (2018)	IES, FUV, ASI
	Increased open flux	●—Milan et al. (2009a)	FUV, ASI
Delayed substorm onset	Enhanced ring current	●—Milan (2009)	ENA, FUV, ASI
Sawtooth	Enhanced O+ outflow	●—Brambles et al. (2011), Ouellette et al. (2013)	ENA, FUV, ASI
	Medium solar wind velocity and southward IMF	●—McPherron et al. (2008), Pulkkinen et al. (2010), Pulkkinen et al. (2007)	IES, MAG, FUV, ASI
	Prolonged southward IMF and enhanced open flux	●—Milan et al. (2019)	MAG, FUV, ASI
Steady magnetospheric convection	Low solar wind velocity and weak southward IMF	●—McPherron et al. (2008), O'Brien (2002), Pulkkinen et al. (2010)	IES, MAG, FUV, ASI
	Prolonged southward IMF	●—Milan et al. (2019), Walach and Milan (2015)	MAG, FUV, ASI
	Substorm	●—Kissinger et al. (2012a)	FUV, ASI
	Increased pressure in the inner-magnetosphere	●—Kissinger et al. (2012b)	ENA, FUV, ASI

includes the solar wind local to the magnetosphere, the microscale auroral dynamics associated with nightside reconnection, and the return of flux to the dayside magnetosphere and subsequent outward motion of the magnetopause boundary. STORM's unique mission design provides all these essential observations.

Isolated substorms (Akasofu, 1964; Akasofu, 2017) require a period of energy storage following southward IMF turnings. These isolated tail modes exhibit a ~1 h growth phase corresponding to plasma sheet thinning and expansion of the auroral oval. This leads to a transient, localized, onset marked by a discrete brightening of the nightside auroral oval in the vicinity of local midnight followed by a ~30 min expansion phase. This expansion phase is characterized by dynamic aurora moving poleward and spanning multiple hours of local time across the night sky. The expansion phase is followed by a ~1 h recovery phase during which aurora dim and the oval begins to expand again. Sawtooth events are sequences of three–eight substorms that occur every ~2–4 h during a nearly continual growth phase (Borovsky et al., 1993; DeJong et al., 2007). Some reports indicate substorm sequences (duration) and properties (auroral brightness and oval motion) during several-daylong geomagnetic storms differ from

those of non-storm time substorms (Baumjohann et al., 1996; Korth et al., 2002; Hoffman et al., 2010) while other reports indicate they do not (Hsu and McPherron, 2000).

Not all nightside reconnection modes follow the isolated substorm sequence. Poleward boundary intensifications (PBI), pseudobreakups, or steady magnetospheric convection (SMC) can occur with no growth, expansion, or recovery phases. PBIs occur as brightenings with ~1° or more longitudinal extent along the most poleward arc (Zesta et al., 2002). They may be the optical signatures of nightside reconnection. The north/south oriented arcs, known as streamers, that ensue are thought to be the optical signatures of reconnection-induced flow bursts. Pseudobreakups occurring on 10 min time scales are auroral brightenings resembling those at substorm onset that do not engage the open field line region within the polar cap (Akasofu, 1964). SMCs are intervals of strongly southward IMF orientation greater than ~6 h long without classical substorms. They exhibit multiple bursts of streamer activity corresponding to bursts of nightside reconnection that, in total, balance steady dayside reconnection (DeJong et al., 2009; Kissinger et al., 2012b; Walach and Milan, 2015).

Table 1 highlights the vast array of observational work, spanning over half a century, dedicated to identifying the drivers of nightside reconnection modes. It also illustrates the often-contradictory findings of these studies regarding the importance of various solar wind and magnetospheric conditions that favor the development of each mode. Although there have been extensive improvements in global simulations, these models frequently produce contradictory results (Gordeev et al., 2017). These contradictions are due to model limitations including, for example, simulations that do not fully couple all relevant plasma regimes, model results that depend on spatiotemporal resolution, and global simulations that do not fully include kinetic effects or realistic ionospheres and thermospheres. These limitations and contradictory results preclude disentangling the drivers shown in Table 1 using global simulations of the solar wind-magnetosphere interaction. STORM provides the observations needed to distinguish between diverse nightside reconnection modes, determine their occurrence patterns as a function of solar wind and geomagnetic conditions, and quantify the significance of each in the global circulation of energy throughout the magnetosphere.

STORM's extended array of high-resolution ground-based imagers together with the global auroral imager distinguish between proposed interaction modes. FUV must observe the nightside electron aurora with a spatial resolution of at least 100 km ($\sim 1^\circ$ latitude) and cadence of 3 min to track the $\sim 5^\circ$ equatorward motion and rapid expansion of the nightside aurora to distinguish each reconnection mode (Frey et al., 2004a). STORM determines whether substorms are isolated, sawtooth, or occurring during geomagnetic storms by their repetition times and the state of geomagnetic activity as measured by the Disturbance-Storm Time (Dst) index. Due to limited ground-based coverage, FUV's global auroral imaging is the only robust method available for identifying long duration events, including SMCs, sawtooth substorms, and geomagnetic storms.

STORM identifies SMC events on the basis of 1) MAG observations of strongly southward IMF orientations, 2) FUV observations of a steady proton aurora in the dayside oval indicative of continuous dayside reconnection (a prerequisite for balanced reconnection), 3) FUV observations of an auroral oval with nearly constant dimensions (thereby requiring the FUV to have a FOV that covers the entire auroral oval), and 4) ASI observations of repetitive auroral streamers. This method of identifying SMCs is superior to those relying on ground-based magnetometers (Kissinger et al., 2011), which can only infer intervals of SMC, as these methods provide no measure of the amount of open flux stored in the magnetosphere. The ASI array complements FUV and must provide observations with spatial resolutions of 20 km and cadences of 30 s to identify auroral streamers (Gallardo-Lacourt et al., 2014) with azimuthal scale sizes of $\sim 0.5^\circ$ – 1.0° that correspond to 25–50 km at geomagnetic latitudes of $\sim 65^\circ$. STORM employs ASI and FUV observations to identify PBIs and pseudobreakups in the nightside auroral oval. Finally, STORM's circular orbit and 30 R_E radius enable its imagers to observe phenomena continuously throughout the various time scales (minutes to days) that encompass all nightside interaction modes, including those of multi-day geomagnetic storms.

STORM determines the occurrence patterns of magnetotail reconnection modes as a function of solar wind and geomagnetic conditions, including solar wind and magnetospheric triggers

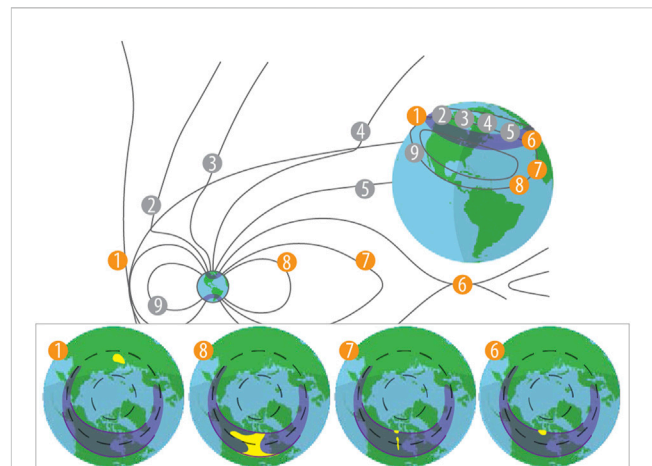


FIGURE 4

STORM's global observations define the flow of energy from the dayside to the magnetotail and back (1–9). This flow of energy can be used to test models in which bursts of dayside reconnection initiate inward magnetopause motion and transient enhancements in the intensity of the dayside proton aurora (1), followed by a nightside PBI (6), auroral streamers (7), and finally substorm onset (8).

(McPherron et al., 2008; DeJong et al., 2009; Walach et al., 2017). The extensive list of proposed drivers for magnetotail reconnection modes (Table 1) demonstrates the need for STORM's proposed observations to test these hypotheses systematically both event and statistical bases. This includes comprehensive end-to-end substorm models such as that proposed by Lyons et al. (2016). As illustrated in Figure 4, this model emphasizes the role of meso-scale features within the global circulation of energy throughout the magnetosphere in triggering substorms. A burst of dayside reconnection causes the dayside auroral oval to jump equatorward and the magnetopause to jump earthward. This burst of dayside reconnection generates a plasma structure that propagates anti-sunward and triggers a PBI along the nightside auroral oval. In turn, the PBI launches an equatorward-moving auroral streamer that initiates substorm onset. STORM is ideally instrumented to test and verify global model predictions for dayside, nightside, and solar wind triggers, or the lack thereof (Zesta et al., 2002; Zesta et al., 2006; Murphy et al., 2014), for various magnetotail modes. This is because STORM uniquely provides observations of the dayside magnetopause and auroral oval locations identifying whether reconnection is steady or bursty, the microscale streamers that may trigger substorm onset, and the global auroral response to geomagnetic substorms. STORM provides MAG and IES observations with at least 1.5 s and 2 min cadences from vantage points near Earth. Note that the performance of existing instruments far exceeding these cadences (Figure 2). Studies have shown that timing accuracy decreases with distance from the magnetosphere (Collier et al., 1998; Richardson and Paularena, 1998; Weimer et al., 2003). Because solar wind features have a variety of scale sizes (Crooker et al., 1982; Richardson and Paularena, 1998; Matsui et al., 2002; Weimer et al., 2003), the probability of observing a feature which will impact the subsolar magnetopause decreases with increasing distance away from the Sun-Earth line. Vantage points near

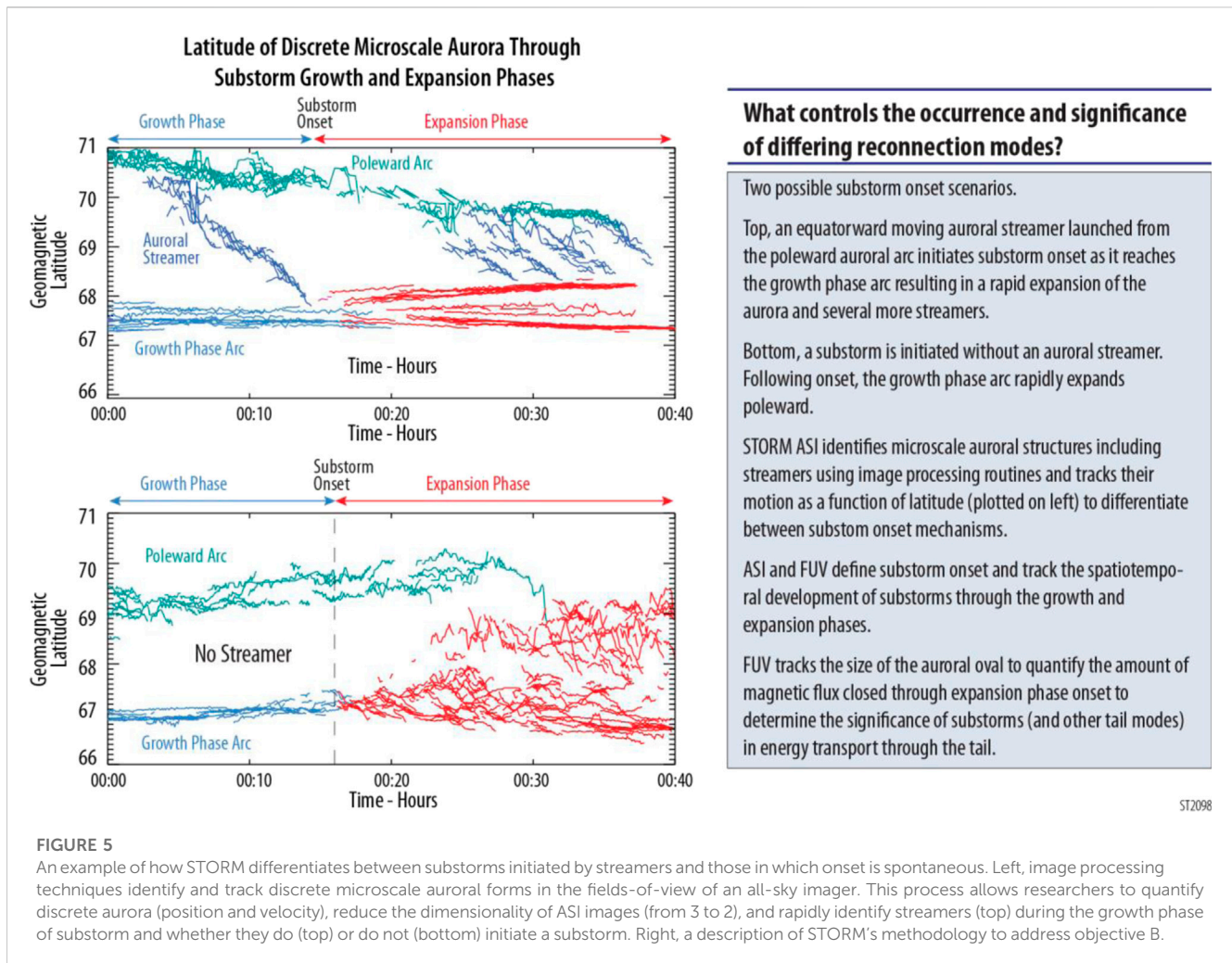


FIGURE 5

An example of how STORM differentiates between substorms initiated by streamers and those in which onset is spontaneous. Left, image processing techniques identify and track discrete microscale auroral forms in the fields-of-view of an all-sky imager. This process allows researchers to quantify discrete aurora (position and velocity), reduce the dimensionality of ASI images (from 3 to 2), and rapidly identify streamers (top) during the growth phase of substorm and whether they do (top) or do not (bottom) initiate a substorm. Right, a description of STORM's methodology to address objective B.

Earth minimize these concerns allowing STORM to determine whether solar wind triggers exist, reach the magnetopause, or initiate substorms with greater amplitudes than those that are not triggered (Lyons, 1996; Hsu and McPherron, 2009).

STORM quantifies the significance of individual magnetotail reconnection modes by determining the amount of open polar cap magnetic flux closed, the strength of inner magnetosphere electric fields, rate of convection, the amount of magnetic flux returned to the dayside magnetosphere, and (on a statistical basis) the occurrence rates of the individual mechanisms for differing solar wind, geomagnetic conditions, and histories. FUV tracks the global dimensions of the electron auroral oval with a resolution of 1° to quantify its size and calculate cross polar potential drops, reconnection rates, and flux closure by nightside reconnection (Milan et al., 2007). Simultaneous XRI and FUV must identify the sunward motion of the magnetopause with $0.25 R_E$ resolution and poleward motion of the dayside auroral oval with 1° resolution to determine if individual modes of nightside reconnection return flux to the dayside (Siscoe et al., 2011) and to quantify the significance of this flux return in the global circulation of energy throughout the magnetosphere. EUV must track the boundary of the plasmasphere with a cadence of 2 min and $0.18 R_E$ resolution to quantify the strength of convection and the driving convective electric fields (Goldstein et al., 2005).

STORM combines unique and comprehensive global space- and ground-based observations to 1) identify distinct modes of magnetotail reconnection, 2) determine their occurrence patterns, and 3) quantify their significance in the circulation of energy throughout the magnetosphere as a function of solar wind and geomagnetic conditions. Figure 5 demonstrates how STORM differentiates between substorms initiated by auroral streamers and those initiated without auroral streamers; case studies and statistics allow STORM to determine the importance of each mode in energy transport through the magnetotail.

3.3 Science objective C: Energy sources and sinks for the ring current

The return of closed magnetic flux to and acceleration and transport of plasma into the inner magnetosphere is the next sequence of energy flow in the Dungey cycle. The acceleration and transport of plasma energizes the ring current and dynamic processes within the inner magnetosphere and on the dayside control the subsequent decay of terrestrial ring current. Science Objective C investigates energy sources and sinks for the ring

current by answering three underlying questions: How efficiently do the magnetotail response modes described in Science Objective B energize ring current ions? How do transport and loss mechanisms affect subsequent evolution of the energized ring current? What are the occurrence patterns of the source, transport, and loss mechanisms?

Ring current ions with energies of 30–300 keV at distances of 4–5 R_E from Earth originate in the Earth's plasma sheet. Each magnetotail reconnection mode: isolated substorms, sawtooth substorms, storm-time substorms, and steady magnetospheric convection (SMC)—supplies ions to the ring current in the form of sequential bursty bulk flows (auroral streamers), substorm injections, and enhanced convection and inner magnetospheric electric fields. Large scale injections associated with isolated substorms provide enhancements by a factor of two to four in the intensity of ~100 keV ions within a pre-midnight wedge with a local time extent that ranges from ~2 to >7 h that can penetrate to within ~4 R_E from Earth (Reeves et al., 1990; Reeves et al., 1991; Reeves et al., 1992; Friedel et al., 1996). Particle injections may penetrate deeper for substorms that consume more magnetic flux (Boakes et al., 2009). Sawtooth and storm-time substorms enhance ring current intensities more effectively than isolated substorms, in part because of the continued and prolonged injection of particles (Reeves and Henderson, 2001) with greater intensities (Cai et al., 2006; Clauer et al., 2006; Walach et al., 2017). However, storm-time and sawtooth modes may inject ions onto open drift paths, leading to only a limited enhancement of the partial ring current in the dusk sector. Prolonged SMC intervals lead to the energization of 5–10 keV ions by factors of up to 10 during ~7 min long traversals from the nightside near $X_{GSE} = -12 R_E$ to locations as close to Earth as $X_{GSE} = -3 R_E$ (Artemyev et al., 2015; Ukhorskiy et al., 2018). These injections result in substantial contributions to the ring current (Gkioulidou et al., 2014).

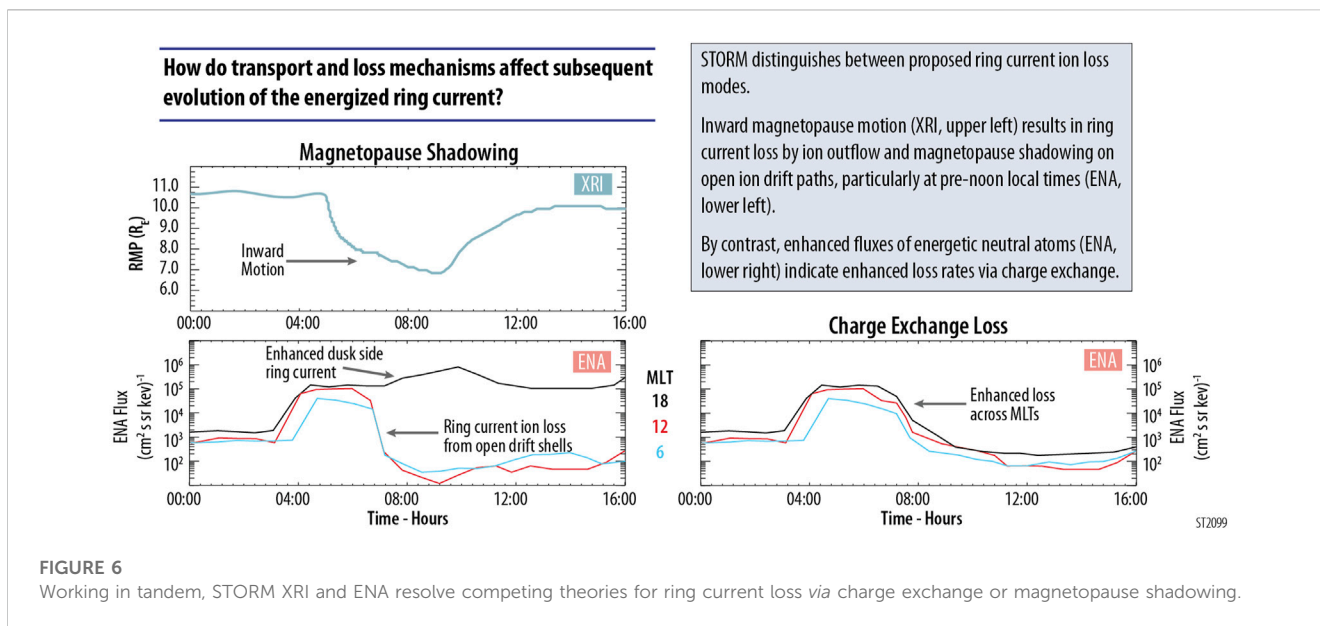
Ring current intensities do not increase indefinitely. During storms ring current intensities initially decay rapidly over ~8 h during the early recovery phase and then more slowly over the next several days (Hamilton et al., 1988). Proposed mechanisms for ring current loss include charge exchange, wave-particle induced precipitation, and magnetopause shadowing/outflow. Daglis et al. (1999) concluded that charge exchange with the exosphere is the main mechanism for ring current decay. The fast initial and subsequent slow decay in ring current intensities may result from the higher charge exchange rate of oxygen and slower charge exchange rate of protons (Hamilton et al., 1988; Jordanova et al., 1996; Jordanova et al., 1998; Daglis et al., 1999). By contrast, Liemohn et al. (1999) maintain that the storm time ring current is a partial ring current on open drift paths from which loss *via* drifts to the magnetopause predominates during periods of enhanced convection. *In-situ* observations suggesting greater ion intensities post-than pre-noon support this hypothesis (Kronberg et al., 2015). As the convection electric field decays during the late recovery phase, the slower charge exchange loss dominates ring current decay on completely closed drift paths (Takahashi et al., 1990; Liemohn et al., 2001). Electromagnetic ion cyclotron (EMIC) wave-particle interactions and precipitation may become important during the main phase of geomagnetic storms (Gonzalez et al., 1989), particularly at low (10 keV) energies where charge exchange cross sections are 70 times greater than those at higher (100 keV) energies

(Smith and Bewtra, 1978; Runov et al., 2016). It is estimated that EMIC wave-driven precipitation accounts for ~1–7% of the ion loss (Kozyra et al., 1997; Jordanova et al., 1998). However, recent work suggests EMIC waves are more widespread than originally thought, especially during the main phase of geomagnetic storms (Usanova et al., 2010; Tetrick et al., 2017), which may also explain the two-stage decay of the ring current during storms. In contrast, Thorne and Horne (Thorne and Horne, 2004) suggest the presence of O^+ in the ring current during the storm main phase limits EMIC wave growth and subsequently any loss *via* EMIC wave-particle interactions.

STORM provides the observations needed to comprehensively evaluate the energization and decay of the ring current (Kozyra and Liemohn, 2003). Section 3.2 addressed how STORM distinguishes between each nightside reconnection mode and quantifies the occurrence and significance of these modes to magnetospheric convection and magnetic flux balance. STORM uses three methods to evaluate the contribution of each nightside mode to the energization of the ring current: 1) ENA tracks the intensity of energetic neutral atoms from the ring current as a function of time to quantify how individual injection events and prolonged intervals of nightside reconnection contribute to the energization of the ring current (Jorgensen et al., 1997). 2) ENA determines the depth to which ring current ion injections penetrate, their azimuthal extent, the degree to which ions are energized, their spectral slopes, and H, O composition on a case-by-case and statistical basis for each event category. 3) EUV tracks the motion of the plasmopause to distinguish between and quantify steady and impulsive electric fields applied to the inner magnetosphere and the resulting magnetospheric convection.

By tracking the time-history of ring current intensities observed by ENA, STORM quantifies the loss rates of ring current ions driven by magnetopause shadowing (West et al., 1972), charge exchange, and precipitation. STORM evaluates the significance of these loss mechanisms in isolation during individual events in three ways: 1) IES observing intervals of enhanced solar wind pressure that compress the magnetopause, making magnetopause shadowing (aka outflow) more likely. As illustrated in Figure 6, the loss rate due to magnetopause shadowing is then determined by comparing pre- and post-noon ENA emissions (Brandt, 2002) on open outer magnetospheric drift paths that originate from and lead to the magnetopause where the location is determined to within 0.25 R_E by XRI observations. 2) ENA directly measuring loss *via* charge exchange as a function of species (H, O), energy, location, and time (Keika et al., 2006). 3) FUV observing precipitation in the proton aurora (Frey et al., 2004b; Fuselier, 2004; Frey, 2007; Spasojevic and Fuselier, 2009; Spasojević et al., 2013) with at least a 100 km spatial resolution to identify the extent and magnitude of scattered ring current ions. ENA tracks the decay in ring current intensities throughout such precipitation events.

Beyond these topics, STORM can test how oxygen may regulate the storage and flow of energy from the magnetotail. Enhanced ionospheric outflow and low energy oxygen in the plasma sheet may result in stronger geomagnetic storms (Glocer et al., 2009). However, enhanced oxygen densities may move the reconnection line closer to Earth, resulting in less heating, less plasma access to the inner magnetosphere, and a weaker ring current (Ilie et al., 2015). ENA provides observations of total ring current and energized oxygen

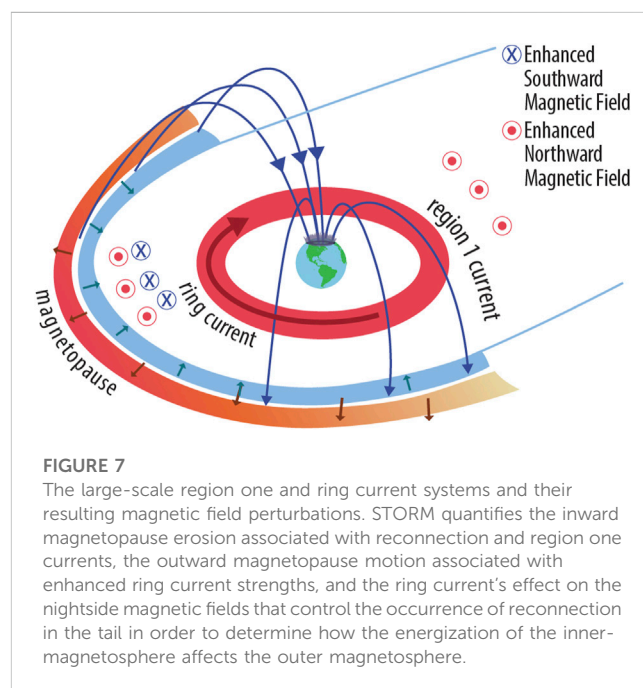


intensities to discriminate between these hypotheses. These energized plasma populations are used to deduce the presence of lower energy outflow and plasma sheet oxygen and thereby determine the overall role of magnetospheric oxygen in controlling the flow of energy in the coupled solar wind-magnetosphere system.

STORM provides continuous observations of the ring current to quantify the sources and sinks of ring current energy. STORM builds on science objective B to distinguish between and quantify how energy is transferred from the nightside magnetotail to the inner magnetosphere in the form of ring current enhancements. STORM quantifies individual ring current ion loss processes, determines their occurrence patterns, and calculates their relative contribution to ring current dynamics. For example, [Figure 6](#) demonstrates how STORM differentiates between magnetopause shadowing and charge exchange losses in the ring current. Finally, although all the instruments on STORM observe many geomagnetic storms from start to finish, these instruments observe even more individual initial, main, and recovery phases, enabling the mission to conduct statistical studies of each phase.

3.4 Science objective D: Energy feedback from the inner magnetosphere

The inner magnetosphere is not the final stop in the circulation of energy in the coupled solar wind-magnetosphere system. Rather the inner magnetosphere hosts dynamic processes that have important feedback effects on the solar wind-magnetosphere interaction. To quantify the circulation of energy in the solar wind-magnetosphere system it is imperative to separate the effects of the solar wind and storage of energy in the tail from the effects of inner magnetospheric plasmas. Science Objective D investigates energy feedback from the inner magnetosphere by answering the following question: How do the ring current and plasmaspheric plumes affect the outer magnetosphere including day



and nightside reconnection and the location of the dayside magnetopause?

Plasmaspheric plumes frequently become entrained in magnetopause reconnection ([McFadden et al., 2008](#)), particularly during geomagnetic storms when plumes persist for days ([Borovsky and Denton, 2008](#)). Since reconnection rates are inversely proportional to plasma densities ([Cassak & Shay, 2007](#)), the arrival of a high density plasmaspheric plume at the magnetopause quenches reconnection. Simulations show that plumes locally reduce the reconnection rate by a factor of 2 ([Borovsky et al., 2008](#)), however this may be compensated for by enhancing reconnection rates at magnetopause locations just

outside the regions where the plumes encounter the magnetopause such that the net dayside reconnection rate remains unchanged (Ouellette et al., 2016).

A strong storm-time ring current that endures from hours to days can affect the dynamics of the dayside and nightside magnetosphere. The ring current enhances northward magnetic field strengths in the dayside and nightside outer magnetosphere, including locations near the magnetopause. As shown in Figure 7, corresponding enhancements in the magnetospheric pressure cause the magnetopause to move outward (Schield, 1969) and compete with the inward erosion of the magnetopause resulting from Region one field-aligned currents associated with reconnection on the dayside magnetopause (Sibeck et al., 1991). Tsyganenko and Sibeck (1994) estimated the effect of the ring current, if any, on the magnetopause location to be small; however, global MHD models with no ring current systematically predict the magnetopause closer to Earth than observed, suggesting the effect of the ring current on magnetopause location is not negligible (García & Hughes, 2007). MHD simulations and simple calculations indicate that even the modest enhancements in ring current strength corresponding to small geomagnetic storms can move the subsolar magnetopause outward by $\sim 0.3\text{--}0.8 R_E$ (Samsonov et al., 2016). Observationally, the results are mixed; Petrinc and Russell (1993) reported that the ring current has only a small effect on the magnetopause location. However, a number of researchers report that enhanced partial ring currents in the dusk magnetosphere cause a clear outward motion of the duskside magnetopause (Wrenn et al., 1981; McComas et al., 1993; Dmitriev et al., 2004; Dmitriev et al., 2005; Dmitriev and Suvorova, 2012), although some researchers dispute this effect (McComas et al., 1994).

In the magnetotail, enhanced northward magnetic fields may prevent the magnetospheric magnetic field from assuming the stretched magnetotail configuration needed to initiate substorms. Consequently, periods of enhanced ring current may require greater amounts of open magnetospheric flux to initiate substorms and also lead to more intense bursts of nightside reconnection (Milan et al., 2009b).

To investigate the effect of plumes on dayside reconnection STORM utilizes EUV to identify plumes and determine their arrival time and location at the magnetopause from their sunward velocity. At geosynchronous orbit, plumes typically have widths of $1\text{--}6 R_E$ and move outward/sunward at velocities of ~ 10 km/s, with the velocity diminishing with age and increasing with the strength of magnetospheric convection (Borovsky and Denton, 2008), placing a requirement on EUV cadence and spatial resolution (10 km/s is $0.5 R_E$ in 10 min). FUV then determines whether plumes halt equatorward erosion of the dayside auroral oval from electron observations and diminish the proton flux precipitating into the high latitude dayside ionosphere from proton aurora observations. XRI further supplements these observations by tracking the magnetopause location, where inward motion due to reconnection should be quenched by the arrival of a plume.

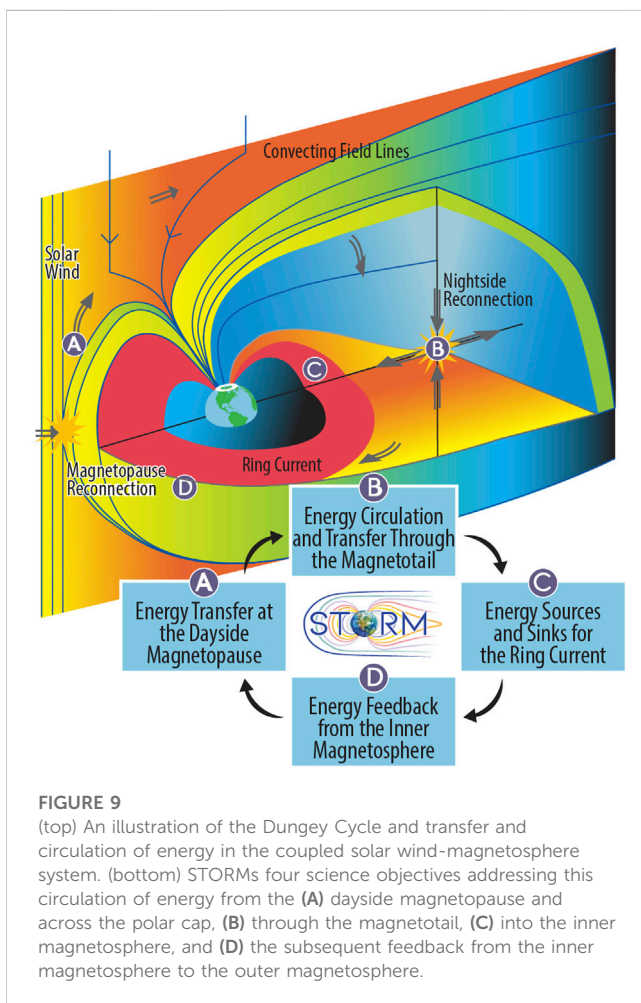
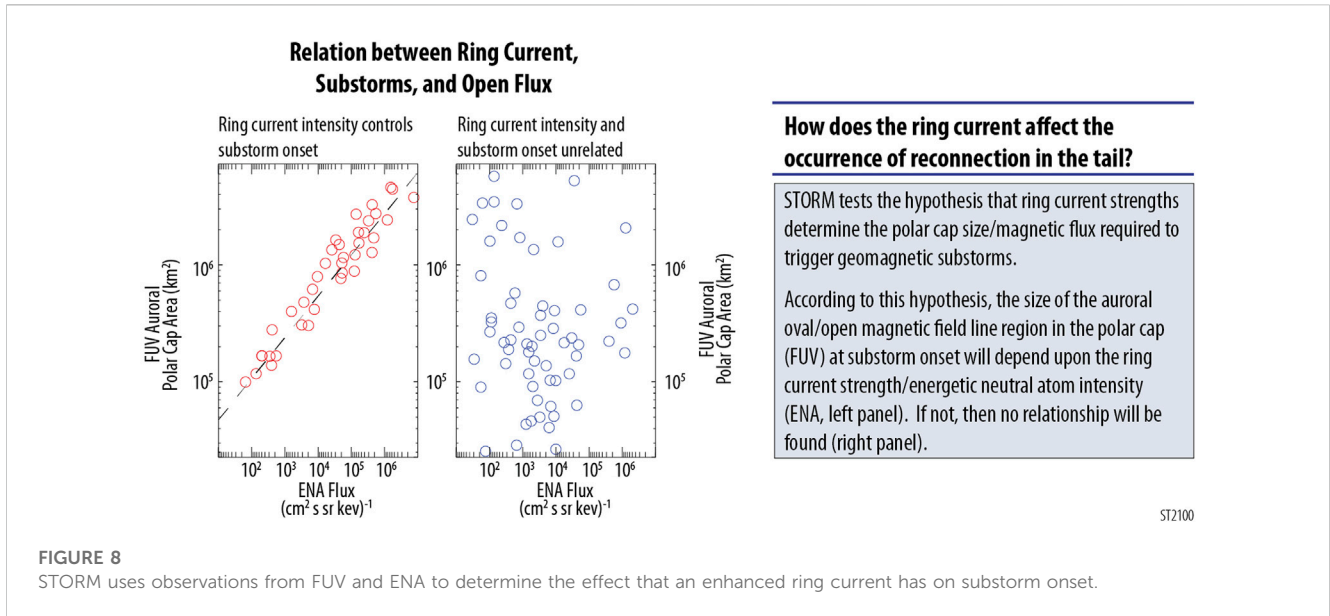
When STORM is located at high latitudes, ENA observes energetic neutral atoms coming from the ring current at all local times and radial distances, enabling direct determination of ring current and partial ring current strengths (Fok et al., 2003) not possible by other observations such as ground-based magnetometers

which observe the integrated effects of several current systems (e.g., the magnetopause, Region 1 and 2, ring current, cross-tail, and electrojet currents) (O'Brien and McPherron, 2000). From similar vantage points, XRI observes the location of the global dayside magnetopause, including outward displacements due to the ring current and dawn/dusk asymmetries resulting from the partial ring current. Working together, ENA and XRI determine whether enhanced ring current strengths push the entire magnetopause outward, and/or whether enhanced partial ring current strengths push the post-noon magnetopause outward. To quantify the effect of the ring current on nightside reconnection, ENA observes variations in ring current strength from equatorial and polar vantage points. When at polar locations, STORM employs FUV to determine the size and shape of the polar cap and therefore the amount of open magnetic flux needed to trigger substorm onset. When STORM is at equatorial latitudes, the ASI array identifies the time and location of substorm onset in a limited local time sector. Working together, these instruments determine whether greater amounts of open flux are needed to trigger substorms during periods when ring current strengths are enhanced (Milan, 2009).

STORM uses simultaneous and global observations of the ring current, plasmasphere, magnetopause, and auroral oval to determine the effects of the ring current and cold plasmaspheric plasma on the dayside and nightside magnetosphere. Images of the ring current, plasmasphere and plumes, magnetopause location, and auroral oval allow STORM to quantify the effect of the ring current and cold plasma on the location of the dayside magnetopause and rate of dayside reconnection, as well as the latitude of substorm onset in the nightside auroral oval. Science Objective D completes STORM's comprehensive investigation and quantitative determination of the circulation of energy throughout the magnetosphere in the coupled solar-wind magnetosphere system. Figure 8 demonstrates how STORM quantitatively tests the relationship between ring current strength and the amount of open flux required to trigger a substorm.

4 Discussion and summary

Heliophysics addresses the complex chain of phenomena that links events on the Sun through the solar wind to responses in the Earth's magnetosphere and ionosphere. Nowhere are the effects of these phenomena felt more keenly than within the Earth's magnetosphere. Here solar wind variations batter the magnetopause, power intense auroral displays, inject energized particles into the inner magnetosphere, and reconfigure the overall morphology of magnetospheric plasma. The solar wind-magnetosphere interaction has practical space weather consequences; especially during geomagnetic storms and substorms. It can push the magnetopause inward below geosynchronous orbit, an indicator of intense geomagnetic activity, and drive powerful currents into the ionosphere in the vicinity of the auroral oval that overwhelm electric power grids and heat the upper atmosphere leading to increased satellite drag. Because of these hazards, understanding the circulation of energy in the solar wind-magnetosphere interaction constitutes a fundamental goal for Heliophysicists.



The past 60 years have seen considerable progress toward this goal. Figure 9 summarizes current understanding of the global solar wind-magnetosphere interaction. Case and

statistical studies show the single most important factor favoring geomagnetic and auroral activity within the magnetosphere is a southward interplanetary magnetic field (IMF) orientation. Inferred from this is that magnetic reconnection dominates the flow of solar wind energy into and through the magnetosphere. Reconnection on the dayside magnetopause opens closed magnetospheric magnetic field lines (Location A in Figure 9), increases the area of open magnetic field lines within the polar caps, causes the auroral oval to expand equatorward, and adds magnetic flux to the magnetotail. Reconnection on the dayside magnetopause and the addition of magnetic flux to the magnetotail cannot continue indefinitely. Reconnection within the magnetotail closes open magnetic field lines (Location B in Figure 9), energizes particles that stream down magnetic field lines causing the contracting auroral oval to brighten, and injects energized plasma sheet ions into the nightside ring current (Location C in Figure 9). Ring current ions may be lost via exchanging charges with exospheric neutrals, precipitating into the Earth's atmosphere, or exiting the magnetosphere (Location D in Figure 9). Feedback effects from the inner magnetosphere can regulate outer magnetospheric processes. The ring current enhances outer magnetospheric magnetic field strengths, pushing the magnetopause outward and inhibiting magnetotail reconnection. The global end-to-end circuit is only complete when the magnetic field lines closed by nightside reconnection return to the dayside magnetosphere.

Most knowledge concerning the nature of the solar wind-magnetosphere interaction has been gained through *in-situ* observations made by isolated spacecraft and ground-based observatories. By their very nature, these observations do not provide the global view necessary to evaluate and quantify the importance of various physical processes to the overall dynamics of the system, except on a statistical basis. For example, it has been established that the dayside magnetopause erodes earthward following a southward IMF turning. Proposed mechanisms

predict steady or unsteady, local or global magnetopause erosion (Section 3.1). By comparison, a bewildering array of solar wind/magnetospheric conditions or triggers have been proposed to favor the various nightside reconnection modes that include isolated substorms, repetitive sawtooth substorms, storm-time substorms, and steady magnetospheric convection events (Section 3.2). The significance of each mode, as measured by its global impact in terms of magnetic flux closure, or ion injections into the ring current, remains to be determined. Deeper within the magnetosphere, the relative significance of ring current loss to charge exchange, precipitation, or magnetopause shadowing/outflow as a function of quiet-time or storm phase is not known with any level of certainty.

Previous missions have laid the groundwork for a clearer understanding of global solar wind-magnetosphere interactions. NASA's Polar and IMAGE missions observed the auroral oval, ring current, and plasmasphere, demonstrating the validity of remote sensing as a technique to track the course of auroral substorms, identify ion injections into the ring current, and determine the convective electric fields applied to the inner magnetosphere. However, several factors precluded these missions from extracting global end-to-end science. They had no XRI instrument to monitor the location and quantify the motion of the magnetopause. In the absence of simultaneous observations of the solar wind input from a nearby solar wind monitor, they could not be certain of the timing or even the arrival of solar wind features, including triggers. They could not attain a global viewpoint that included the crucial dynamics of the magnetopause where reconnection occurs and energy enters the magnetosphere. They were unable to achieve perspectives from all vantage points as needed to deduce the 3-dimensional structure of magnetospheric plasma regimes. No previous mission could make observations continually throughout geomagnetic storms as all were in highly elliptical orbits that periodically passed through perigee. And, they could not turn to a dedicated array of ground-based imagers for simultaneous measurements of the microstructures in the nightside auroral oval that reflect magnetotail processes believed to play a crucial role in substorm initiation.

Numerical simulations, including global magnetohydrodynamic (MHD), ring current, and particle-in-cell hybrid codes, enable visualizations of how individual solar wind-magnetosphere interaction modes modify magnetospheric configurations, thereby creating diagnostic signatures in plasma regime morphologies. Due to model limitations these models cannot be used to develop a complete understanding of the solar wind-magnetospheric interaction and the physical processes which control the dynamics of this interaction. However, they can be used to predict the response of the magnetosphere for comparison to observations.

STORM would be the first self-standing mission to observe the solar wind input and image the magnetopause in conjunction with other global plasma structures, and thereby resolve the circulation of energy that governs the solar wind's interaction with the magnetosphere. STORM will observe the sequence and signatures of global end-to-end energy circulation over the entirety of geomagnetic storms to test competing theories for dayside reconnection, magnetotail energy release, as well as particle

acceleration and particle loss in the inner magnetosphere as discussed below. STORM would not rely on distant L1 solar wind monitors, reducing concerns about the scale size and arrival times of solar wind features reaching Earth's magnetopause. STORM answers key questions that past *in-situ* and remote sensing missions and simulations have raised but were unable to answer. STORM quantitatively evaluates the significance of each proposed interaction mode by quantifying both its amplitude/extent and occurrence rate, with the significance then defined as the product of these (Section 3).

STORM's Magnetometer (MAG) and Ion Electron Spectrometer (IES) measure the solar wind in the vicinity of the magnetosphere along streamlines more likely to encounter the magnetopause than those observed by L1 monitors. STORM's soft X-Ray Imager (XRI) identifies and tracks the motion of the dayside magnetopause in response to erosion and solar wind pressure variations. The Far UltraViolet spectroscopy (FUV) determines when and where reconnection enables protons to precipitate into the dayside auroral oval, the location and extent of the open magnetic field line region within the polar cap, the time of auroral substorm onset, and the occurrence of subauroral ring current ion precipitation. A dedicated array of ground-based All-Sky imagers (ASI) in Alaska and Canada complements the FUV observations by providing high spatial and temporal resolution observations of the microscale auroral features that many researchers believe reflect processes that trigger geomagnetic substorms and/or constitute steady magnetospheric convection events. The Energetic Neutral Atom (ENA) imager observes the plasma sheet and tracks the intensity of the ring current and partial ring current. The Extreme Ultraviolet (EUV) imager tracks the plasmapause, intensity/density of the plasmasphere, and formation and dynamics of plumes. Working together, the imagers identify and track the locations of plasma boundaries and magnetospheric transients as they respond to varying solar wind conditions.

Imaging the global magnetosphere from all vantage points throughout the course of a 2-year mission that includes events lasting from hours to several days requires STORM to orbit the Earth in a highly-inclined circular orbit with a period of 9.65 days at a radius of $30 R_E$. This orbit enables the XRI to observe a broad region of the dayside magnetopause while not compromising the spatial resolutions with which the FUV, ENA, and EUV instruments image their targets. This orbit intentionally places the spacecraft in the near-Earth solar wind for days at a time, at locations where IES and MAG observe the solar wind input into the magnetosphere at cadences relevant to the global interaction throughout major disturbances such as geomagnetic storms.

Beyond STORM's four science objectives, STORM offers unique opportunities for the community to address science topics not covered in Section 3. These include but are not limited to:

- (1) Determining the three-dimensional structure of the plasma regimes such as the bow shock, magnetopause, ring current, and storm-time plasma sheet
- (2) Imaging magnetopause waves driven by the Kelvin-Helmholtz instability and solar wind buffeting
- (3) Examining the magnetopause and magnetospheric plasma response to interplanetary shocks

- (4) Examining XRI soft X-ray observations to identify the species of charge exchange signatures of high-charge-state solar wind ions within magnetospheric plasma
- (5) Employing *in-situ* MAG and IES observations to explore the physics of the nightside magnetopause, bow shock, and magnetotail
- (6) Quantifying the ionospheric energy budget from observations of auroral intensities
- (7) Examining spatial distribution and temporal evolution of exospheric neutrals
- (8) Using STORMs *in-situ* particle and magnetometer instruments to improve space weather forecasting, and investigate and quantify the error resulting from use of L1 and propagated L1 observations in space weather and magnetospheric research

As designed, STORM is uniquely positioned to collaborate with all concurrent solar, magnetospheric, and ionospheric missions. STORM extends observations from missions studying the Sun (such as the recently selected PUNCH mission) elucidating how solar wind structures, including CMEs and CIRs, interact with the Earth's magnetosphere. STORM determines the nature of dayside reconnection intervals, complementing low-altitude cusp observations such as those that will be provided the recently selected TRACERS SmEx mission. STORM provides the energy budget into the ionosphere for missions focused on the ITM system such as GOLD and ICON, to quantify and understand the variability of the ionosphere and the effects the magnetosphere has on the ionosphere. Finally, STORM provides global observations of the magnetosphere to understand local dynamics observed *in-situ* by spacecraft such as the NASA MMS and THEMIS missions, the GOES and LANL spacecraft, the AMPERE-2 project and other future magnetospheric missions.

Joint work between STORM and the new AMPERE-2 project is particularly valuable to the Heliophysics community. Together, STORM and AMPERE-2 address the two key objectives of the proposed MEDICI mission outlined in the 2013 Heliophysics Decadal Survey (Baker et al., 2013): 1) How are magnetospheric and ionospheric plasmas transported and accelerated by solar wind forcing and by magnetosphere-ionosphere (M-I) coupling processes? and 2) How do magnetospheric and ionospheric plasma pressures and currents drive cross-scale electric and magnetic fields, which then affect the plasma dynamics? STORM provides crucial information concerning the solar wind drivers, the nature of the dayside and nightside interactions, and precipitation into the ionosphere. AMPERE-2 provides information on the response of the magnetospheric currents needed to understand their feedback on auroral and ring current plasma structures. Finally, STORM would work in conjunction with the forthcoming GDC mission by providing observations of the solar input into the magnetosphere system and global images of the aurora for quantifying magnetosphere-ionosphere coupling. STORM's spaceborne imagers, *in-situ* plasma and magnetic field instruments, and array of ASIs provide the first system science view of the solar wind-magnetosphere interaction for days at a time from all vantage points.

Overall, STORM comprehensively tracks the end-to-end circulation of energy throughout the solar wind-magnetosphere system by systematically addressing four sequentially linked science objectives: A) energy transfer at the dayside magnetopause, B) energy circulation and transfer through the magnetotail, C) energy sources and sinks for the ring current, and D) energy feedback from the inner magnetosphere. STORM's strategic mission design provides the pathway to understanding the solar wind-magnetosphere system as a whole, its constituent parts, and its cross-scale processes on a continuous basis, as needed to quantify the flow of solar wind energy through the global magnetospheric system and fills a critical gap in NASA's Heliophysics System Observatory as a strategic self-standing system science mission.

Data availability statement

The original contributions presented in the study are included in the article/supplementary material, further inquiries can be directed to the corresponding author.

Author contributions

All authors contributed to the development and design of the STORM mission concept including science objectives and requirements and mission design. DGS and KRM were responsible for compiling the article and article figures.

Funding

This work was partially supported by Phase A funding from the NASA Explorer Office and JSPS KAKENHI Grant Numbers JP17KK0097, JP19H00727. HU Frey was partially supported by NASA grant 80NSSC20K0218. RTD was supported by STFC Ernest Rutherford Fellowship ST/W004801/1.

Conflict of interest

The authors declare that the research was conducted in the absence of any commercial or financial relationships that could be construed as a potential conflict of interest.

Publisher's note

All claims expressed in this article are solely those of the authors and do not necessarily represent those of their affiliated organizations, or those of the publisher, the editors and the reviewers. Any product that may be evaluated in this article, or claim that may be made by its manufacturer, is not guaranteed or endorsed by the publisher.

References

- Akasofu, S. I. (2017). Auroral substorms: Search for processes causing the expansion phase in terms of the electric current approach. *Space Sci. Rev.* 212 (1–2), 341–381. doi:10.1007/s11214-017-0363-7
- Akasofu, S. I. (1964). The development of the auroral substorm. *Planet. Space Sci.* 12 (4), 273–282. doi:10.1016/0032-0633(64)90151-5
- Artemyev, A. V., Liu, J., Angelopoulos, V., and Runov, A. (2015). Acceleration of ions by electric field pulses in the inner magnetosphere. *J. Geophys. Res. Space Phys.* 120 (6), 4628–4640. doi:10.1002/2015JA021160
- Aubry, M. P., Russell, C. T., and Kivelson, M. G. (1970). Inward motion of the magnetopause before a substorm. *J. Geophys. Res.* 75 (34), 7018–7031. doi:10.1029/JA075i034p07018
- Baker, D. N., Fritz, T. A., Lennartsson, W., Wilken, B., Kroehl, H. W., and Birn, J. (1985). The role of heavy ionospheric ions in the localization of substorm disturbances on march 22, 1979: Cdaw 6. *J. Geophys. Res.* 90 (A2), 1273. doi:10.1029/JA090iA02p01273
- Baker, D. N., and Pulkkinen, T. I. (1997). Energy requirement of magnetic reconnection during magnetospheric substorms. *Adv. Space Res.* 19 (12), 1923–1927. doi:10.1016/S0273-1177(97)00102-6
- Baumjohann, W., Kamide, Y., and Nakamura, R. (1996). Substorms, storms, and the near-earth tail. *J. Geomagnetism Geoelectr.* 48 (2), 177–185. doi:10.5636/jgg.48.177
- Boakes, P. D., Milan, S. E., Abel, G. A., Freeman, M. P., Chisham, G., and Hubert, B. (2009). A statistical study of the open magnetic flux content of the magnetosphere at the time of substorm onset. *Geophys. Res. Lett.* 36 (4), L04105. doi:10.1029/2008GL037059
- Boakes, P. D., Milan, S. E., Abel, G. A., Freeman, M. P., Chisham, G., Hubert, B., et al. (2008). On the use of IMAGE FUV for estimating the latitude of the open/closed magnetic field line boundary in the ionosphere. *Ann. Geophys.* 26 (9), 2759–2769. doi:10.5194/angeo-26-2759-2008
- Borovsky, J. E., and Denton, M. H. (2008). A statistical look at plasmaspheric drainage plumes. *J. Geophys. Res. Space Phys.* 113 (A9), n/a. doi:10.1029/2007ja012994
- Borovsky, J. E., Hesse, M., Birn, J., and Kuznetsova, M. M. (2008). What determines the reconnection rate at the dayside magnetosphere? *J. Geophys. Res. Space Phys.* 113 (A7), n/a. doi:10.1029/2007ja012645
- Borovsky, J. E., Nemzek, R. J., and Belian, R. D. (1993). The occurrence rate of magnetospheric-substorm onsets: Random and periodic substorms. *J. Geophys. Res. Space Phys.* 98 (A3), 3807–3813. doi:10.1029/92JA02556
- Brambles, O. J., Lotko, W., Zhang, B., Wiltberger, M., Lyon, J., and Strangeway, R. J. (2011). Magnetosphere sawtooth oscillations induced by ionospheric outflow. *Science* 332 (6034), 1183–1186. doi:10.1126/science.1202869
- Brandt, P. C. (2002). Global IMAGE/HENA observations of the ring current: Examples of rapid response to IMF and ring current-plasmasphere interaction. *J. Geophys. Res.* 107 (A11), 1359. doi:10.1029/2001JA000084
- Burch, J. L. (1972). Precipitation of low-energy electrons at high latitudes: Effects of interplanetary magnetic field and dipole tilt angle. *J. Geophys. Res.* 77 (34), 6696–6707. doi:10.1029/JA077i034p06696
- Caan, M. N., McPherron, R. L., and Russell, C. T. (1978). The statistical magnetic signature of magnetospheric substorms. *Planet. Space Sci.* 26 (3), 269–279. doi:10.1016/0032-0633(78)90092-2
- Cai, X., Clauer, C. R., and Ridley, A. J. (2006). Statistical analysis of ionospheric potential patterns for isolated substorms and sawtooth events. *Ann. Geophys.* 24 (7), 1977–1991. doi:10.5194/angeo-24-1977-2006
- Cameron, T., and Jackel, B. (2016). Quantitative evaluation of solar wind time-shifting methods. *Space weather.* 14 (11), 973–981. doi:10.1002/2016SW001451
- Cassak, P. A., and Shay, M. A. (2007). Scaling of asymmetric magnetic reconnection: General theory and collisional simulations. *Phys. Plasmas* 14 (10), 102114. doi:10.1063/1.2795630
- Clauer, C. R., Cai, X., Welling, D., DeJong, A., and Henderson, M. G. (2006). Characterizing the 18 April 2002 storm-time sawtooth events using ground magnetic data. *J. Geophys. Res.* 111 (A4), A04S90. doi:10.1029/2005JA011099
- Collier, M. R., and Connor, H. K. (2018). Magnetopause surface reconstruction from tangent vector observations. *J. Geophys. Res. Space Phys.* 123 (12), 2018JA025763. doi:10.1029/2018JA025763
- Collier, M. R., Slavin, J. A., Lepping, R. P., Szabo, A., and Ogilvie, K. (1998). Timing accuracy for the simple planar propagation of magnetic field structures in the solar wind. *Geophys. Res. Lett.* 25 (14), 2509–2512. doi:10.1029/98GL00735
- Connor, H. K., Sibeck, D. G., Collier, M. R., Baliukin, I. I., Branduardi-Raymont, G., Brandt, P. C., et al. (2021). Soft X-ray and ENA imaging of the Earth's dayside magnetosphere. *J. Geophys. Res. Space Phys.* 126 (3), e2020JA028816. doi:10.1029/2020JA028816
- Crooker, N. U. (1979). Dayside merging and cusp geometry. *J. Geophys. Res.* 84 (A3), 951. doi:10.1029/JA084iA03p0951
- Crooker, N. U., Siscoe, G. L., Russell, C. T., and Smith, E. J. (1982). Factors controlling degree of correlation between ISEE 1 and ISEE 3 interplanetary magnetic field measurements. *J. Geophys. Res.* 87 (4), 2224. doi:10.1029/JA087iA04p02224
- Daglis, I. A., Thorne, R. M., Baumjohann, W., and Orsini, S. (1999). The terrestrial ring current: Origin, formation, and decay. *Rev. Geophys.* 37 (4), 407–438. doi:10.1029/1999RG900009
- DeJong, A. D., Cai, X., Clauer, R. C., and Spann, J. F. (2007). Aurora and open magnetic flux during isolated substorms, sawteeth, and SMC events. *Ann. Geophys.* 25 (8), 1865–1876. doi:10.5194/angeo-25-1865-2007
- DeJong, A. D., Ridley, A. J., Cai, X., and Clauer, C. R. (2009). A statistical study of BRIs (SMCs), isolated substorms, and individual sawtooth injections. *J. Geophys. Res. Space Phys.* 114 (A8), n/a. doi:10.1029/2008ja013870
- Dmitriev, A., Chao, J.-K., Thomsen, M., and Suvorova, A. (2005). Geosynchronous magnetopause crossings on 29–31 October 2003. *J. Geophys. Res. Space Phys.* 110 (A8). doi:10.1029/2004JA010582
- Dmitriev, A., and Suvorova, A. (2012). Equatorial trench at the magnetopause under saturation. *J. Geophys. Res. Space Phys.* 117 (A8), n/a. doi:10.1029/2012ja017834
- Dmitriev, A. V., Suvorova, A. V., Chao, J. K., and Yang, Y. -H. (2004). Dawn-dusk asymmetry of geosynchronous magnetopause crossings. *J. Geophys. Res.* 109 (A5), A05203. doi:10.1029/2003JA010171
- Dungey, J. W. (1961). Interplanetary magnetic field and the auroral zones. *Phys. Rev. Lett.* 6 (2), 47–48. doi:10.1103/PhysRevLett.6.47
- Fear, R. C., Milan, S. E., Fazakerley, A. N., Owen, C. J., Asikainen, T., Taylor, M. G. G. T., et al. (2007). Motion of flux transfer events: A test of the cooling model. *Ann. Geophys.* 25 (7), 1669–1690. doi:10.5194/angeo-25-1669-2007
- Fok, M.-C., Moore, T. E., Brandt, P. C., Delcourt, D. C., Slinker, S. P., and Fedder, J. A. (2006). Impulsive enhancements of oxygen ions during substorms. *J. Geophys. Res.* 111 (A10), A10222. doi:10.1029/2006JA011839
- Fok, M.-C., Moore, T. E., Wilson, G. R., Perez, J. D., Zhang, X. X., Brandt, P. C., et al. (2003). Global ena image simulations. *Space Sci. Rev.* 109 (1–4), 77–103. doi:10.1023/B:SPAC.0000007514.56380.f0
- Forsyth, C., Watt, C. E. J., Rae, I. J., Fazakerley, A. N., Kalmoni, N. M. E., Freeman, M. P., et al. (2014). Increases in plasma sheet temperature with solar wind driving during substorm growth phases. *Geophys. Res. Lett.* 41 (24), 8713–8721. doi:10.1002/2014GL026240
- Freeman, M. P., and Morley, S. K. (2004). A minimal substorm model that explains the observed statistical distribution of times between substorms. *Geophys. Res. Lett.* 31 (12). doi:10.1029/2004gl019989
- Frey, H. U., Haerendel, G., Mende, S. B., Forrester, W. T., Immel, T. J., and Østgaard, N. (2004a). Subauroral morning proton spots (SAMPS) as a result of plasmapause-ring-current interaction. *J. Geophys. Res.* 109 (A10), A10305. doi:10.1029/2004JA010516
- Frey, H. U., Han, D., Kataoka, R., Lessard, M. R., Milan, S. E., Nishimura, Y., et al. (2019). Dayside aurora. *Space Sci. Rev.* 215 (8), 51. doi:10.1007/s11214-019-0617-7
- Frey, H. U. (2007). Localized aurora beyond the auroral oval. *Rev. Geophys.* 45 (1), RG1003. doi:10.1029/2005RG000174
- Frey, H. U., Mende, S. B., Angelopoulos, V., and Donovan, E. F. (2004b). Substorm onset observations by IMAGE-FUV. *J. Geophys. Res.* 109 (A10), A10304. doi:10.1029/2004JA010607
- Frey, H. U., Phan, T. D., Fuselier, S. A., and Mende, S. B. (2003). Continuous magnetic reconnection at Earth's magnetopause. *Nature* 426 (6966), 533–537. doi:10.1038/nature02084
- Friedel, R. H. W., Korth, A., and Kremser, G. (1996). Substorm onsets observed by CRRES: Determination of energetic particle source regions. *J. Geophys. Res. Space Phys.* 101 (A6), 13137–13154. doi:10.1029/96JA00399
- Fuselier, S. A. (2004). Generation of transient dayside subauroral proton precipitation. *J. Geophys. Res.* 109 (A12), A12227. doi:10.1029/2004JA010393
- Gallardo-Lacourt, B., Nishimura, Y., Lyons, L. R., Zou, S., Angelopoulos, V., Donovan, E., et al. (2014). Coordinated SuperDARN THEMIS ASI observations of mesoscale flow bursts associated with auroral streamers. *J. Geophys. Res. Space Phys.* 119 (1), 142–150. doi:10.1002/2013JA019245
- Gallardo-Lacourt, B., Nishimura, Y., Lyons, L. R., and Donovan, E. (2012). External triggering of substorms identified using modern optical versus geosynchronous particle data. *Ann. Geophys.* 30 (4), 667–673. doi:10.5194/angeo-30-667-2012
- García, K. S., and Hughes, W. J. (2007). Finding the Lyon-fedder-mobarry magnetopause: A statistical perspective. *J. Geophys. Res. Space Phys.* 112 (A6). doi:10.1029/2006JA012039
- Gkioulidou, M., Ukhorskiy, A. Y., Mitchell, D. G., Sotiirelis, T., Mauk, B. H., and Lanzerotti, L. J. (2014). The role of small-scale ion injections in the buildup of Earth's ring current pressure: Van Allen Probes observations of the 17 March 2013 storm. *J. Geophys. Res. Space Phys.* 119 (9), 7327–7342. doi:10.1002/2014JA020096

- Glocer, A., Tóth, G., Gombosi, T., and Welling, D. (2009). Modeling ionospheric outflows and their impact on the magnetosphere, initial results. *J. Geophys. Res. Space Phys.* 114 (5). doi:10.1029/2009ja014053
- Goldstein, J., Burch, J. L., Sandel, B. R., Mende, S. B., Cson Brandt, P., and Hairston, M. R. (2005). Coupled response of the inner magnetosphere and ionosphere on 17 April 2002. *J. Geophys. Res. Space Phys.* 110 (A3), A03205. doi:10.1029/2004JA010712
- Goldstein, J., Sandel, B. R., Forrester, W. T., and Reiff, P. H. (2003). IMF-driven plasmasphere erosion of 10 July 2000. *Geophys. Res. Lett.* 30 (3), 1146. doi:10.1029/2002gl016478
- Goldstein, J., and Sandel, B. R. (2005). The global pattern of evolution of plasmaspheric drainage plumes. *Geophys. Monogr. Ser.* 159, 1–22. doi:10.1029/159GM02
- Gonzalez, W. D., Tsurutani, B. T., Gonzalez, A. L. C., Smith, E. J., Tang, F., and Akasofu, S.-I. (1989). Solar wind-magnetosphere coupling during intense magnetic storms (1978–1979). *J. Geophys. Res.* 94 (A7), 8835. doi:10.1029/JA094iA07p08835
- Gordeev, E., Sergeev, V., Merkin, V., and Kuznetsova, M. (2017). On the origin of plasma sheet reconfiguration during the substorm growth phase. *Geophys. Res. Lett.* 44 (17), 8696–8702. doi:10.1002/2017GL074539
- Grande, M., Perry, C. H., Hall, A., Fennell, J., and Wilken, B. (1999). Statistics of substorm occurrence in storm and non-storm periods. *Phys. Chem. Earth, Part C Sol. Terr. Planet. Sci.* 24 (1–3), 167–172. doi:10.1016/S1464-1917(98)00025-7
- Hamilton, D. C., Gloeckler, G., Ipavich, F. M., Stüdemann, W., Wilken, B., and Kremser, G. (1988). Ring current development during the great geomagnetic storm of February 1986. *J. Geophys. Res.* 93 (A12), 14343. doi:10.1029/JA093iA12p14343
- Hoffman, R. A., Gjerloev, J. W., Frank, L. A., and Sigwarth, J. W. (2010). Are there optical differences between storm-time substorms and isolated substorms? *Ann. Geophys.* 28 (5), 1183–1198. doi:10.5194/angeo-28-1183-2010
- Hsu, T.-S. (2002). An evaluation of the statistical significance of the association between northward turnings of the interplanetary magnetic field and substorm expansion onsets. *J. Geophys. Res.* 107 (A11), 1398. doi:10.1029/2000JA000125
- Hsu, T.-S., and McPherron, R. L. (2009). A statistical study of the spatial structure of interplanetary magnetic field substorm triggers and their associated magnetic response. *J. Geophys. Res. Space Phys.* 114 (A2), n/a. doi:10.1029/2008ja013439
- Hsu, T. S., and McPherron, R. L. (2000). “The characteristics of storm-time substorms and non-storm substorms,” in Proceedings of the Fifth International Conference on Substorms, St. Petersburg, Russia, 16–20 May 2000.
- Ilie, R., Liemohn, M. W., Toth, G., Yu Ganushkina, N., and Daldorff, L. K. S. (2015). Assessing the role of oxygen on ring current formation and evolution through numerical experiments. *J. Geophys. Res. Space Phys.* 120 (6), 4656–4668. doi:10.1002/2015JA021157
- Jordanova, V. K., Farrugia, C. J., Quinn, J. M., Thorne, R. M., Ogilvie, K. E., Lepping, R. P., et al. (1998). Effect of wave-particle interactions on ring current evolution for January 10–11, 1997: Initial results. *Geophys. Res. Lett.* 25 (15), 2971–2974. doi:10.1029/98GL00649
- Jordanova, V. K., Kistler, L. M., Kozyra, J. U., Khazanov, G. V., and Nagy, A. F. (1996). Collisional losses of ring current ions. *J. Geophys. Res. Space Phys.* 101 (A1), 111–126. doi:10.1029/95JA02000
- Jorgensen, A. M., Spence, H. E., Henderson, M. G., Reeves, G. D., Sugiura, M., and Kamei, T. (1997). Global energetic neutral atom (ENA) measurements and their association with the dst index. *Geophys. Res. Lett.* 24 (24), 3173–3176. doi:10.1029/97GL03095
- Jorgensen, A. M., Sun, T., Wang, C., Dai, L., Sembay, S., Wei, F., et al. (2019b). Boundary detection in three dimensions with application to the SMILE mission: The effect of photon noise. *J. Geophys. Res. Space Phys.* 124 (6), 4365–4383. doi:10.1029/2018JA025919
- Jorgensen, A. M., Sun, T., Wang, C., Dai, L., Sembay, S., Zheng, J., et al. (2019a). Boundary detection in three dimensions with application to the SMILE mission: The effect of model-fitting noise. *J. Geophys. Res. Space Phys.* 124 (6), 4341–4355. doi:10.1029/2018JA026124
- Kameda, S., Ikezawa, S., Sato, M., Kuwabara, M., Osada, N., Murakami, G., et al. (2017). Ecliptic North-south symmetry of hydrogen geocorona. *Geophys. Res. Lett.* 44 (2311), 11,706–11,712. doi:10.1002/2017GL075915
- Keika, K., Nosé, M., Brandt, P. C., Ohtani, S., Mitchell, D. G., and Roelof, E. C. (2006). Contribution of charge exchange loss to the storm time ring current decay: IMAGE/HENA observations. *J. Geophys. Res.* 111 (A11), A11S12. doi:10.1029/2006JA011789
- Kissinger, J., McPherron, R. L., Hsu, T.-S., Angelopoulos, V., and Chu, X. (2012b). Necessity of substorm expansions in the initiation of steady magnetospheric convection. *Geophys. Res. Lett.* 39 (15), L15105. doi:10.1029/2012GL052599
- Kissinger, J., McPherron, R. L., Hsu, T.-S., and Angelopoulos, V. (2012a). Diversion of plasma due to high pressure in the inner magnetosphere during steady magnetospheric convection. *J. Geophys. Res. Space Phys.* 117 (A5). doi:10.1029/2012ja017579
- Kissinger, J., McPherron, R. L., Hsu, T.-S., and Angelopoulos, V. (2011). Steady magnetospheric convection and stream interfaces: Relationship over a solar cycle. *J. Geophys. Res. Space Phys.* 116 (A5). doi:10.1029/2010JA015763
- Knipp, D. J., Emery, B. A., Engebretson, M., Li, X., McAllister, A. H., Mukai, T., et al. (1998). An overview of the early November 1993 geomagnetic storm. *J. Geophys. Res. Space Phys.* 103 (A11), 26197–26220. doi:10.1029/98JA00762
- Korth, A., Friedel, R. H. W., Frutos-Alfaro, F., Mouikis, C. G., and Zong, Q. (2002). Ion composition of substorms during storm-time and non-storm-time periods. *J. Atmos. Solar-Terrestrial Phys.* 64 (5–6), 561–566. doi:10.1016/S1364-6826(02)00013-5
- Koskinen, H. E. J. (2002). Magnetospheric energy budget and the epsilon parameter. *J. Geophys. Res.* 107 (A11), 1415. doi:10.1029/2002JA009283
- Kozyra, J. U., Jordanova, V. K., Home, R. B., and Thorne, R. M. (1997). Modeling of the contribution of electromagnetic ion cyclotron (EMIC) waves to stormtime ring current erosion. Washington, DC: American Geophysical Union, 187–202. doi:10.1029/GM098p0187
- Kozyra, J. U., and Liemohn, M. W. (2003). Ring current energy input and decay. *Space Sci. Rev.* 109 (1–4), 105–131. doi:10.1023/B:SPAC.0000007516.10433.ad
- Kronberg, E. A., Grigorenko, E. E., Haaland, S. E., Daly, P. W., Delcourt, D. C., Luo, H., et al. (2015). Distribution of energetic oxygen and hydrogen in the near-Earth plasma sheet. *J. Geophys. Res. Space Phys.* 120 (5), 3415–3431. doi:10.1002/2014JA020882
- Le, G., Russell, C. T., and Kuo, H. (1993). Flux transfer events: Spontaneous or driven? *Geophys. Res. Lett.* 20 (9), 791–794. doi:10.1029/93GL00850
- Liemohn, M. W., Kozyra, J. U., Jordanova, V. K., Khazanov, G. V., Thomsen, M. F., and Cayton, T. E. (1999). Analysis of early phase ring current recovery mechanisms during geomagnetic storms. *Geophys. Res. Lett.* 26 (18), 2845–2848. doi:10.1029/1999GL900611
- Liemohn, M. W., Kozyra, J. U., Thomsen, M. F., Roeder, J. L., Lu, G., Borovsky, J. E., et al. (2001). Dominant role of the asymmetric ring current in producing the stormtime Dst. *J. Geophys. Res. Space Phys.* 106 (A6), 10883–10904. doi:10.1029/2000JA000326
- Lockwood, M., Cowley, S. W. H., Sandholt, P. E., and Lepping, R. P. (1990). The ionospheric signatures of flux transfer events and solar wind dynamic pressure changes. *J. Geophys. Res.* 95 (A10), 17113. doi:10.1029/JA095iA10p17113
- Lockwood, M., Lanchester, B. S., Frey, H. U., Throp, K., Morley, S. K., Milan, S. E., et al. (2003). IMF control of cusp proton emission intensity and dayside convection: Implications for component and anti-parallel reconnection. *Ann. Geophys.* 21 (4), 955–982. doi:10.5194/angeo-21-955-2003
- Lockwood, M., Sandholt, P. E., Cowley, S. W. H., and Oguti, T. (1989). Interplanetary magnetic field control of dayside auroral activity and the transfer of momentum across the dayside magnetopause. *Planet. Space Sci.* 37 (11), 1347–1365. doi:10.1016/0032-0633(89)90106-2
- Lyons, L. R., Lee, D.-Y., Wang, C.-P., and Mende, S. B. (2005). Global auroral responses to abrupt solar wind changes: Dynamic pressure, substorm, and null events. *J. Geophys. Res. Space Phys.* 110 (A8). doi:10.1029/2005JA011089
- Lyons, L. R., Nishimura, Y., Shi, Y., Zou, S., Kim, H.-J., Angelopoulos, V., et al. (2010). Substorm triggering by new plasma intrusion: Incoherent-scatter radar observations. *J. Geophys. Res. Space Phys.* 115 (A7). doi:10.1029/2009JA015168
- Lyons, L. R., Nishimura, Y., and Zou, Y. (2016). Unsolved problems: Mesoscale polar cap flow channels’ structure, propagation, and effects on space weather disturbances. *J. Geophys. Res. Space Phys.* 121 (4), 3347–3352. doi:10.1002/2016JA022437
- Lyons, L. R. (1996). Substorms: Fundamental observational features, distinction from other disturbances, and external triggering. *J. Geophys. Res. Space Phys.* 101 (A6), 13011–13025. doi:10.1029/95JA01987
- Marchaudon, A., Cerisier, J.-C., Bosquet, J.-M., Dunlop, M. W., Wild, J. A., Décréau, P. M. E., et al. (2004). Transient plasma injections in the dayside magnetosphere: One-to-one correlated observations by cluster and SuperDARN. *Ann. Geophys.* 22 (1), 141–158. doi:10.5194/angeo-22-141-2004
- Matsui, H., Farrugia, C. J., and Torbert, R. B. (2002). Wind-ACE solar wind correlations, 1999: An approach through spectral analysis. *J. Geophys. Res.* 107 (A11), 1355. doi:10.1029/2002JA009251
- McComas, D. J., Bame, S. J., Barraclough, B. L., Donart, J. R., Elphic, R. C., Gosling, J. T., et al. (1993). Magnetospheric plasma analyzer: Initial three-spacecraft observations from geosynchronous orbit. *J. Geophys. Res. Space Phys.* 98 (A8), 13453–13465. doi:10.1029/93JA00726
- McComas, D. J., Elphic, R. C., Moldwin, M. B., and Thomsen, M. F. (1994). Plasma observations of magnetopause crossings at geosynchronous orbit. *J. Geophys. Res.* 99 (A11), 21249. doi:10.1029/94JA01094
- McFadden, J. P., Carlson, C. W., Larson, D., Bonnelli, J., Mozer, F. S., Angelopoulos, V., et al. (2008). Structure of plasmaspheric plumes and their participation in magnetopause reconnection: First results from THEMIS. *Geophys. Res. Lett.* 35 (17), L17S10. doi:10.1029/2008GL033677
- McPherron, R. L., Weygand, J. M., and Hsu, T.-S. (2008). Response of the Earth’s magnetosphere to changes in the solar wind. *J. Atmos. Solar-Terrestrial Phys.* 70 (2–4), 303–315. doi:10.1016/j.jastp.2007.08.040
- Milan, S. E. (2009). Both solar wind-magnetosphere coupling and ring current intensity control of the size of the auroral oval. *Geophys. Res. Lett.* 36 (18), L18101. doi:10.1029/2009GL039997

- Milan, S. E., Grocott, A., Forsyth, C., Imber, S. M., Boakes, P. D., and Hubert, B. (2009a). A superposed epoch analysis of auroral evolution during substorm growth, onset and recovery: Open magnetic flux control of substorm intensity. *Ann. Geophys.* 27 (2), 659–668. doi:10.5194/angeo-27-659-2009
- Milan, S. E., Hutchinson, J., Boakes, P. D., and Hubert, B. (2009b). Influences on the radius of the auroral oval. *Ann. Geophys.* 27 (7), 2913–2924. doi:10.5194/angeo-27-2913-2009
- Milan, S. E., Imber, S. M., Carter, J. A., Walach, M. T., and Hubert, B. (2016). What controls the local time extent of flux transfer events? *J. Geophys. Res. Space Phys.* 121 (2), 1391–1401. doi:10.1002/2015JA022112
- Milan, S. E., Lester, M., Cowley, S. W. H., and Brittnacher, M. (2000). Convection and auroral response to a southward turning of the IMF: Polar UVI, CUTLASS, and IMAGE signatures of transient magnetic flux transfer at the magnetopause. *J. Geophys. Res. Space Phys.* 105 (A7), 15741–15755. doi:10.1029/2000JA900022
- Milan, S. E., Provan, G., and Hubert, B. (2007). Magnetic flux transport in the Dungey cycle: A survey of dayside and nightside reconnection rates. *J. Geophys. Res. Space Phys.* 112 (A1), n/a. doi:10.1029/2006ja011642
- Milan, S. E., Walach, M. T., Carter, J. A., Sangha, H., and Anderson, B. J. (2019). Substorm onset latitude and the steadiness of magnetospheric convection. *J. Geophys. Res. Space Phys.* 124 (3), 1738–1752. doi:10.1029/2018JA025969
- Mozer, F. S., Bale, S. D., and Phan, T. D. (2002). Evidence of diffusion regions at a subsolar magnetopause crossing. *Phys. Rev. Lett.* 89, 015002. doi:10.1103/PhysRevLett.89.015002
- Murphy, K. R., Mann, I. R., Rae, I. J., Walsh, A. P., and Frey, H. U. (2014). Inner magnetospheric onset preceding reconnection and tail dynamics during substorms: Can substorms initiate in two different regions? *J. Geophys. Res. Space Phys.* 119 (12), 9684–9701. doi:10.1002/2014JA019795
- Newell, P. T., and Liou, K. (2011). Solar wind driving and substorm triggering. *J. Geophys. Res. Space Phys.* 116 (A3), A03229. doi:10.1029/2010JA016139
- Nishimura, Y., Lyons, L. R., Angelopoulos, V., Kikuchi, T., Zou, S., and Mende, S. B. (2011). Relations between multiple auroral streamers, pre-onset thin arc formation, and substorm auroral onset. *J. Geophys. Res. Space Phys.* 116 (A9), n/a. doi:10.1029/2011ja016768
- Nowada, M., Lin, C.-H., Pu, Z.-Y., Fu, S.-Y., Angelopoulos, V., Carlson, C. W., et al. (2012). Substorm-like magnetospheric response to a discontinuity in the B x component of interplanetary magnetic field. *J. Geophys. Res. Space Phys.* 117 (A4), n/a. doi:10.1029/2011ja016894
- O'Brien, T. P., and McPherron, R. L. (2000). Forecasting the ring current index Dst in real time. *J. Atmos. Solar-Terrestrial Phys.* 62 (14), 1295–1299. doi:10.1016/S1364-6826(00)00072-9
- O'Brien, T. P. (2002). Steady magnetospheric convection: Statistical signatures in the solar wind and AE. *Geophys. Res. Lett.* 29 (7), 1130. doi:10.1029/2001GL014641
- Oksavik, K., Moen, J., Carlson, H. C., Greenwald, R. A., Milan, S. E., Lester, M., et al. (2005). Multi-instrument mapping of the small-scale flow dynamics related to a cusp auroral transient. *Ann. Geophys.* 23 (7), 2657–2670. doi:10.5194/angeo-23-2657-2005
- Oksavik, K., Moen, J., and Carlson, H. C. (2004). High-resolution observations of the small-scale flow pattern associated with a poleward moving auroral form in the cusp. *Geophys. Res. Lett.* 31 (11). doi:10.1029/2004gl019838
- Østgaard, N. (2002). A relation between the energy deposition by electron precipitation and geomagnetic indices during substorms. *J. Geophys. Res.* 107 (A9), 1246. doi:10.1029/2001JA002003
- Ouellette, J. E., Brambles, O. J., Lyon, J. G., Lotko, W., and Rogers, B. N. (2013). Properties of outflow-driven sawtooth substorms. *J. Geophys. Res. Space Phys.* 118 (6), 3223–3232. doi:10.1002/jgra.50309
- Ouellette, J. E., Lyon, J. G., Brambles, O. J., Zhang, B., and Lotko, W. (2016). The effects of plasmaspheric plumes on dayside reconnection. *J. Geophys. Res. Space Phys.* 121 (5), 4111–4118. doi:10.1002/2016JA022597
- Petrinec, S. M., and Russell, C. T. (1993). External and internal influences on the size of the dayside terrestrial magnetosphere. *Geophys. Res. Lett.* 20 (5), 339–342. doi:10.1029/93GL00085
- Pfau-Kempf, Y., Palmroth, M., Johlander, A., Turc, L., Alho, M., Battarbee, M., et al. (2020). Hybrid-Vlasov modeling of three-dimensional dayside magnetopause reconnection. *Phys. Plasmas* 27 (9), 092903. doi:10.1063/5.0020685
- Phan, T., Frey, H. U., Frey, S., Peticolas, L., Fuselier, S., Carlson, C., et al. (2003). Simultaneous Cluster and IMAGE observations of cusp reconnection and auroral proton spot for northward IMF. *Geophys. Res. Lett.* 30 (10). doi:10.1029/2003gl016885
- Pulkkinen, T. I., Goodrich, C. C., and Lyon, J. G. (2007). Solar wind electric field driving of magnetospheric activity: Is it velocity or magnetic field? *Geophys. Res. Lett.* 34 (21), L21101. doi:10.1029/2007GL031011
- Pulkkinen, T. I., Palmroth, M., Koskinen, H. E. J., Laitinen, T. V., Goodrich, C. C., Merkin, V. G., et al. (2010). Magnetospheric modes and solar wind energy coupling efficiency. *J. Geophys. Res. Space Phys.* 115 (A3). doi:10.1029/2009ja014737
- Reeves, G. D., Belian, R. D., and Fritz, T. A. (1991). Numerical tracing of energetic particle drifts in a model magnetosphere. *J. Geophys. Res. Space Phys.* 96 (A8), 13997–14008. doi:10.1029/91ja01161
- Reeves, G. D., Fritz, T. A., Cayton, T. E., and Belian, R. D. (1990). Multi-satellite measurements of the substorm injection region. *Geophys. Res. Lett.* 17 (11), 2015–2018. doi:10.1029/GL017011p02015
- Reeves, G. D., and Henderson, M. G. (2001). The storm-substorm relationship: Ion injections in geosynchronous measurements and composite energetic neutral atom images. *J. Geophys. Res. Space Phys.* 106 (A4), 5833–5844. doi:10.1029/2000ja003017
- Reeves, G. D., Kettmann, G., Fritz, T. A., and Belian, R. D. (1992). Further investigation of the CDAW 7 substorm using geosynchronous particle data: Multiple injections and their implications. *J. Geophys. Res.* 97 (A5), 6417. doi:10.1029/91ja03103
- Richardson, J. D., and Paularena, K. I. (1998). The orientation of plasma structure in the solar wind. *Geophys. Res. Lett.* 25 (12), 2097–2100. doi:10.1029/98GL01520
- Rostoker, G. (1983). Triggering of expansive phase intensifications of magnetospheric substorms by northward turnings of the interplanetary magnetic field. *J. Geophys. Res.* 88 (A9), 6981–6993. doi:10.1029/JA088iA09p06981
- Runov, A., Zhang, X. J., and Angelopoulos, V. (2016). Evolution of partial ring current ion pitch angle distributions during the main phase of a storm on 17 March 2015. *J. Geophys. Res. Space Phys.* 121 (6), 5284–5293. doi:10.1002/2016JA022391
- Russell, C. T., and Elphic, R. C. (1978). Initial ISEE magnetometer results: Magnetopause observations. *Space Sci. Rev.* 22 (6), 681–715. doi:10.1007/BF00212619
- Samsonov, A. A., Gordeev, E., Tsyganenko, N. A., Šafránková, J., Němeček, Z., Šimůnek, J., et al. (2016). Do we know the actual magnetopause position for typical solar wind conditions? *J. Geophys. Res. A Space Phys.* 121 (7), 6493–6508. doi:10.1002/2016JA022471
- Sandholt, P. E., and Farrugia, C. J. (2003). Does the aurora provide evidence for the occurrence of antiparallel magnetopause reconnection? *J. Geophys. Res. Space Phys.* 108 (A12), 1466. doi:10.1029/2003JA010066
- Sandholt, P. E., Farrugia, C. J., Moen, J., and Cowley, S. W. H. (1998). Dayside auroral configurations: Responses to southward and northward rotations of the interplanetary magnetic field. *J. Geophys. Res. Space Phys.* 103 (A9), 20279–20295. doi:10.1029/98ja01541
- Sandhu, J. K., Rae, I. J., Freeman, M. P., Forsyth, C., Gkioulidou, M., Reeves, G. D., et al. (2018). Energization of the ring current by substorms. *J. Geophys. Res. Space Phys.* 123 (10), 8131–8148. doi:10.1029/2018JA025766
- Schild, M. A. (1969). Pressure balance between solar wind and magnetosphere. *J. Geophys. Res.* 74 (5), 1275–1286. doi:10.1029/ja074i005p01275
- Schildge, J. P., and Siscoe, G. L. (1970). A correlation of the occurrence of simultaneous sudden magnetospheric compressions and geomagnetic bay onsets with selected geophysical indices. *J. Atmos. Terr. Phys.* 32 (11), 1819–1830. doi:10.1016/0021-9169(70)90139-X
- Shoemaker, M., Folta, D., and Sibeck, D. (2022). “Application of tisserand’s criterion and the lidov-kozai effect to STORM’s trajectory design,” in 2022 AAS/AIAA Astrodynamic Specialist Conference, Charlotte, North Carolina, August 7–11 2022.
- Sibeck, D. G., Allen, R., Aryan, H., Bodewits, D., Brandt, P., Branduardi-Raymont, G., et al. (2018). Imaging plasma density structures in the soft X-rays generated by solar wind charge exchange with neutrals. *Space Sci. Rev.* 214, 79. doi:10.1007/s11214-018-0504-7
- Sibeck, D. G., Lopez, R. E., and Roelof, E. C. (1991). Solar wind control of the magnetopause shape, location, and motion. *J. Geophys. Res.* 96 (A4), 5489. doi:10.1029/90JA02464
- Siscoe, G. L., Farrugia, C. J., and Sandholt, P. E. (2011). Comparison between the two basic modes of magnetospheric convection. *J. Geophys. Res. Space Phys.* 116 (5), A05210. doi:10.1029/2010JA015842
- Smith, P. H., and Bewtra, N. K. (1978). Charge exchange lifetimes for ring current ions. *Space Sci. Rev.* 22 (3), 301–318. doi:10.1007/BF00239804
- Sonnerup, B. U. Ö. (1974). Magnetopause reconnection rate. *J. Geophys. Res.* 79 (10), 1546–1549. doi:10.1029/ja079i010p01546
- Sonnerup, B. U. Ö., Paschmann, G., Papamastorakis, I., Sckopke, N., Haerendel, G., Bame, S. J., et al. (1981). Evidence for magnetic field reconnection at the Earth’s magnetopause. *J. Geophys. Res.* 86 (A12), 10049. doi:10.1029/ja086i12p10049
- Spasojević, M., and Fuselier, S. A. (2009). Temporal evolution of proton precipitation associated with the plasmaspheric plume. *J. Geophys. Res. Space Phys.* 114 (12). doi:10.1029/2009ja014530
- Spasojević, M., Thomsen, M. R., Chi, P. J., and Sandel, B. R. (2013). “Afternoon subauroral proton precipitation resulting from ring current-plasmasphere interaction,” in *Inner magnetosphere interactions: New perspectives from imaging*. Editors J. Burch, M. Schulz, and H. Spence Hoboken: Wiley. 85–99. doi:10.1029/159GM06
- Sun, T., Wang, C., Connor, H. K., Jorgensen, A. M., and Sembay, S. (2020). Deriving the magnetopause position from the soft X-ray image by using the tangent fitting approach. *J. Geophys. Res. Space Phys.* 125 (9), e2020JA028169. doi:10.1029/2020JA028169
- Takahashi, S., Iyemori, T., and Takeda, M. (1990). A simulation of the storm-time ring current. *Planet. Space Sci.* 38 (9), 1133–1141. doi:10.1016/0032-0633(90)90021-H

- Tetrick, S. S., Engebretson, M. J., Posch, J. L., Olson, C. N., Smith, C. W., Denton, R. E., et al. (2017). Location of intense electromagnetic ion cyclotron (EMIC) wave events relative to the plasmapause: Van Allen Probes observations. *J. Geophys. Res. Space Phys.* 122 (4), 4064–4088. doi:10.1002/2016JA023392
- Thorne, R. M., and Horne, R. B. (2004). Modulation of electromagnetic ion cyclotron instability due to interaction with ring current O⁺ during magnetic storms. *J. Geophys. Res. Space Phys.* 102 (A7), 14155–14163. doi:10.1029/96ja04019
- Trattner, K. J., Fuselier, S. A., Petrinec, S. M., Burch, J. L., Ergun, R., and Grimes, E. W. (2021). Long and active magnetopause reconnection X-lines during changing IMF conditions. *J. Geophys. Res. Space Phys.* 126 (4), e2020JA028926. doi:10.1029/2020JA028926
- Tsyganenko, N. A., and Sibeck, D. G. (1994). Concerning flux erosion from the dayside magnetosphere. *J. Geophys. Res.* 99 (A7), 13425. doi:10.1029/94ja00719
- Ukhorskiy, A. Y., Sorathia, K. A., Merkin, V. G., Sitnov, M. I., Mitchell, D. G., and Gkioulidou, M. (2018). Ion trapping and acceleration at dipolarization fronts: High-resolution MHD and test-particle simulations. *J. Geophys. Res. Space Phys.* 123 (7), 5580–5589. doi:10.1029/2018JA025370
- Usanova, M. E., Mann, I. R., Kale, Z. C., Rae, I. J., Sydora, R. D., Sandanger, M., et al. (2010). Conjugate ground and multisatellite observations of compression-related EMIC Pc1 waves and associated proton precipitation. *J. Geophys. Res. Space Phys.* 115 (A7). doi:10.1029/2009ja014935
- Vorobjev, V. G., Yagodkina, O. I., Antonova, E. E., and Zverev, V. L. (2018). Influence of solar wind plasma parameters on the intensity of isolated magnetospheric substorms. *Geomagnetism Aeronomy* 58 (3), 295–306. doi:10.1134/s0016793218030155
- Walach, M. T., and Milan, S. E. (2015). Are steady magnetospheric convection events prolonged substorms? *J. Geophys. Res. Space Phys.* 120 (3), 1751–1758. doi:10.1002/2014JA020631
- Walach, M. T., Milan, S. E., Murphy, K. R., Carter, J. A., Hubert, B. A., and Grocott, A. (2017). Comparative study of large-scale auroral signatures of substorms, steady magnetospheric convection events, and sawtooth events. *J. Geophys. Res. Space Phys.* 122 (6), 6357–6373. doi:10.1002/2017JA023991
- Weimer, D. R., Ober, D. M., Maynard, N. C., Collier, M. R., McComas, D. J., Ness, N. F., et al. (2003). Predicting interplanetary magnetic field (IMF) propagation delay times using the minimum variance technique. *J. Geophys. Res.* 108 (A1), 1026. doi:10.1029/2002JA009405
- West, H. I., Buck, R. M., and Walton, J. R. (1972). Shadowing of electron azimuthal-drift motions near the noon magnetopause. *Nat. Phys. Sci.* 240 (97), 6–7. doi:10.1038/physci240006a0
- Wrenn, G. L., Johnson, J. F. E., Norris, A. J., and Smith, M. F. (1981). Geos-2 magnetopause encounters: Low energy (<500 eV) particle measurements. *Adv. Space Res.* 1 (1), 129–134. doi:10.1016/0273-1177(81)90096-X
- Zesta, E., Donovan, E., Lyons, L., Enno, G., Murphree, J. S., and Cogger, L. (2002). Two-dimensional structure of auroral poleward boundary intensifications. *J. Geophys. Res. Space Phys.* 107 (A11), 1350. doi:10.1029/2001JA000260
- Zesta, E., Lyons, L., Wang, C. P., Donovan, E., Frey, H., and Nagai, T. (2006). Auroral poleward boundary intensifications (PBIs): Their two-dimensional structure and associated dynamics in the plasma sheet. *J. Geophys. Res. Space Phys.* 111 (5), A05201. doi:10.1029/2004JA010640
- Zou, Y., Walsh, B. M., Chen, L., Ng, J., Shi, X., Wang, C., et al. (2022). Unsteady magnetopause reconnection under quasi-steady solar wind driving. *Geophys. Res. Lett.* 49 (1), e2021GL096583. doi:10.1029/2021GL096583